

YALE PEABODY MUSEUM

P.O. BOX 208118 | NEW HAVEN CT 06520-8118 USA | PEABODY.YALE. EDU

JOURNAL OF MARINE RESEARCH

The *Journal of Marine Research*, one of the oldest journals in American marine science, published important peer-reviewed original research on a broad array of topics in physical, biological, and chemical oceanography vital to the academic oceanographic community in the long and rich tradition of the Sears Foundation for Marine Research at Yale University.

An archive of all issues from 1937 to 2021 (Volume 1–79) are available through EliScholar, a digital platform for scholarly publishing provided by Yale University Library at <https://elischolar.library.yale.edu/>.

Requests for permission to clear rights for use of this content should be directed to the authors, their estates, or other representatives. The *Journal of Marine Research* has no contact information beyond the affiliations listed in the published articles. We ask that you provide attribution to the *Journal of Marine Research*.

Yale University provides access to these materials for educational and research purposes only. Copyright or other proprietary rights to content contained in this document may be held by individuals or entities other than, or in addition to, Yale University. You are solely responsible for determining the ownership of the copyright, and for obtaining permission for your intended use. Yale University makes no warranty that your distribution, reproduction, or other use of these materials will not infringe the rights of third parties.



This work is licensed under a Creative Commons Attribution-NonCommercial-ShareAlike 4.0 International License.
<https://creativecommons.org/licenses/by-nc-sa/4.0/>



Modeling the variability of the Somali Current

by D.L.T. Anderson¹, D.J. Carrington¹, R. Corry¹ and C. Gordon¹

ABSTRACT

The dynamics of the Somali Current system during the southwest Monsoon are investigated using a 16 level general circulation model. Solutions are found for a number of model geometries and wind-forcing patterns. The first integrations reported use a model domain exactly equivalent to that of the layer model of McCreary and Kundu allowing a direct comparison between the level and layer models. In the second set of integrations a more realistic Indian Ocean geometry is used, but still with an idealized wind forcing, while in the third, the Hellerman and Rosenstein wind stresses are used to simulate the seasonal cycle.

The main results are that the GCM does not easily produce the cold wedge observed in SST at $\sim 4\text{N}$, although a current separation does develop there. A cold wedge can be produced but only if there is cold water quite close to the surface, the SST being sensitive to the vertical temperature profile. The cold wedge at $\sim 10\text{N}$ forms easily in all integrations. As the water flows offshore it slides beneath the surface giving rise to the impression that it corkscrews its way around the Great Whirl gyre. To the east, northeast, of the Great Whirl, a series of jet filaments develop, associated with strong vertical circulations. In broad outline the GCM and layer model of MK are similar, but the details of the eddy fields and coastal response are quite different. In no cases are there vacillations or gyre interactions comparable to those in the layer model.

1. Introduction

The rapid changes which occur in the Somali Current on a seasonal basis have made this a region of special interest to dynamical modellers. The spectacular changes are most evident following the end of the northeast monsoon, and so it is the summer evolution of the Somali Current which has received most attention, and in particular the upper ocean flow. The fully-developed Somali Current of northern summer is a major western boundary current with transports in the upper 200 m of the order of $60 \times 10^6 \text{m}^3 \text{s}^{-1}$ (Swallow and Bruce, 1966) and surface velocities reaching 3.7ms^{-1} (Düing, Molinari and Swallow, 1980). Results from the International Indian Ocean Expedition (IIOE) of 1964 emphasised a more or less continuous flow along the coast to a separation and offshore recirculation at about 9–10N, called the 'Great Whirl' by Findlay (1866) and denoted A in Figure 1. In addition, there was evidence

1. Robert Hooke Institute, Clarendon Laboratory, Parks Road, Oxford, OX1 3PU, England.

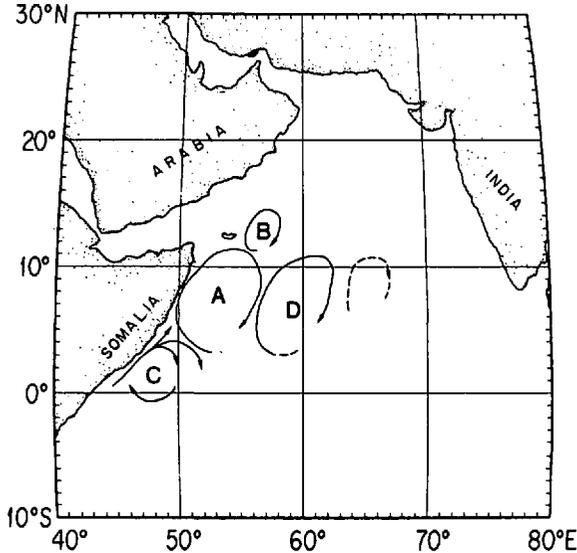


Figure 1. Schematic showing the Great Whirl (A), the Socotra eddy (B) and the Southern 'gyre' (C). From Bruce 1981.

of a clockwise gyre farther north that was distinguishable from the Great Whirl by salinity, now called the Socotra Eddy denoted B on Figure 1. It would appear from the higher salinity of the Socotra Eddy that it is of Arabian Sea origin, whereas the Great Whirl has fresher water at least in the later part of the summer indicative of water from a more southern origin.

More recent studies, notably from FGGE (1979), indicate that the flow south of the Great Whirl is more complicated and that there may not be a continuous coastal current. Bruce (1973) was the first to suggest a separation at a lower latitude as well as a northern separation, and to point out that there were substantial changes within a season as well as between years. His double separation idea was based on hydrographic measurements from the Chain Cruise of August-September 1970. Anderson and Rowlands (1976) also proposed a low-latitude separation, based on results from a linear model and some UK Met. Office monthly-mean ship-drift currents. These indicated a separation at a lower latitude (about 4N) with this more evident earlier in the southwest monsoon than in the later stages. Such a structure (i.e. a coastal current that crossed the equator but turned offshore in the vicinity of 4N) was noted again in Bruce (1979). The separation at 4N is taken as the northern expression of a gyre denoted C in Figure 1, though the flow may merge with the equatorial current system rather than forming a closed circulation. The year of the major Indian Ocean Experiment (INDEX), 1979, was a two-gyre year and a more complete (though still far from comprehensive) set of observations was obtained. Swallow and Fieux (1982), from an analysis of historical data for the period

1900–1973 found the two-gyre system to be the norm, a result supported by the recent modelling studies of Luther and O'Brien (1989).

The picture that has emerged is that the two-gyre structure may be a transient feature. In June there is a major eddy, the Great Whirl, probably spun-up locally between 5N and 10N, and to the south there is a fresher flow which crosses the equator and separates at 4N. Part of this flow may recirculate. As the current evolves, the southern separation becomes less noticeable and by late in the monsoon (late August) the coastal flow is largely continuous with no marked southern separation. The separations at about 4N and at about 10N both have a thermal expression in the sea surface temperature (SST). A cold water wedge exists between the two gyres, and also on the northern flank of the Great Whirl. By late in the monsoon (August) the gyres identified during INDEX merged in a process which was not well resolved by *in situ* measurements, but fairly clearly indicated by satellite images which showed a northward migration of the southern cold water wedge associated with the southern separation point (Schott, 1983). This merger marked a transition to a single separation (9N) with northward flow all along the coast, as was found at a similar stage of the 1964 monsoon by IIOE investigators. It also resulted in low salinity water moving northward into the Great Whirl, again in accord with the 1964 finding of a salinity contrast between the Great Whirl and the more northern Socotra Eddy late in the monsoon.

Various models of eddies in the Somali Current have appeared to explain the measurements. Most rely on wind forcing as the primary forcing mechanism. Hurlbert and Thomson (1976) in a single-layer reduced-gravity model with a coast aligned north-south, simulated eddies generated just north of the equator which propagated smoothly and steadily northward along the coast. The evidence from the INDEX experiment does not support steady movement of gyres but rather that the two gyres remain fixed for much of the time, and then coalesce only during August. Cox (1979) in a multi-level general circulation model (GCM) also found a succession of eddies when the coast was aligned north-south, but when he rotated the boundary to lie from southwest to northeast the model yielded a two-eddy system with offshore turnings in about the right places. The location of the gyres was however sensitive to the numerical scheme used and to the nature of the boundary conditions (free or no-slip applied along the Somali coast). Another interesting and at first sight counter-intuitive result found by Cox is that, for stronger wind stress, the flow separated at lower latitudes. This is presumably because the southern eddy is driven by shear flow, and the stronger the stress, the earlier and hence at lower latitude an eddy can be formed. Cox's studies however did not really give a clear indication of how the gyres interact. In fact the evidence from FGGE, 1979, is that there are two gyres, largely fixed in location until mid-August, when according to Brown *et al.* (1980) there is a rather rapid coalescence (within one or possibly two weeks). According to Schott (1983) the process leading to the rapid movement of the

southern gyre does not appear to be clearly related to the weakening of the southwest monsoon since, in two of the three years Schott analyzed, the northward migration of the southern gyre started well before the southwest monsoon weakened. Schott (1983) questions that the gyres always coalesce and suggests that at least sometimes the southern gyre nudges the Great Whirl away as it moves northward.

More recently, Luther and O'Brien (1989) have modelled the Somali Current using a high resolution model forced by realistic winds and with geometry representative of the Western Indian Ocean. They have performed a 23 year integration using winds from 1954 to 1976 to force a reduced gravity model (resolution of $\frac{1}{4}^\circ$ zonally and $\frac{1}{2}^\circ$ meridionally). They find that the two-gyre structure of the Somali region occurs in 21 of the 23 years. In 14 of the 21 years, the two gyres coalesce in July–August, while in the remaining 7, the southern gyre did not move northward. A quasi-biennial signal is noted in the model during the period 1954 to 1966, but not during the period 1967 to 1975. Higher frequency motion is also observed: 40/50 day variability in February through April in the region to the north of Madagascar, and 26 day waves on the equator away from the western boundary. We are not concerned directly with this high frequency variability in this paper but the interested reader will find significant discussion in the papers of Schott *et al.* (1988), Kindle and Thompson (1989) and Woodberry *et al.* (1989). By running their model using seasonally-varying climatological winds as opposed to the 23 year 'real' wind case Luther and O'Brien were able to identify those regions in which there is internal variability in the ocean as opposed to variability resulting from the wind forcing. The regions of internal model variability are limited to the above-mentioned regions and to small-scale features on the Great Whirl.

This result is contradictory to that of McCreary and Kundu (1988), hereafter denoted MK, who suggest that there is vacillation in the Somali gyre system from a two-gyre to a single-gyre state. They use a $2\frac{1}{2}$ layer model with a simple parameterization of thermodynamics similar to that of Anderson and McCreary (1985), but with an improved parameterization of mixed-layer processes. The geometry and winds used are idealized, but they produce interesting results. In particular, the model exhibits vacillation, most evident when forced with a wind-patch chosen to represent the region of strong alongshore winds associated with the Findlater Jet (Findlater, 1971) in the northern part of the Somali coast. Based on their results, MK conclude that a double-gyre state is not a possible equilibrium response to the peak phase of the southwest monsoon. The Southern gyre must move northward and coalesce with the Great Whirl, followed by a southward movement of the single super-gyre. Further, if the wind is maintained for a period extending beyond the end of the southwest monsoon, the model vacillates between one- and two-gyre states. In this scenario, the southern gyre moves northward and coalesces with the northern

gyre. This single gyre then moves southward. A new gyre forms to the north and moves south to become the new Great Whirl and so on.

Of course a direct comparison with data is not possible since in reality the winds do not continue unabated. In an experiment in which the winds are weakened MK find that the Great Whirl just decays and breaks up very quickly (within about 20 days). They argue that the existence of vacillation could give rise to interannual variability, not associated with interannual variability in the wind but arising from internal ocean dynamics. We would like to test the ideas that the double-gyre is not a possible equilibrium response to the monsoon peak, that the two gyres must interact to form a super-gyre and that if the winds continued beyond the end of the southwest monsoon there would be vacillation between one and two-gyre states. In particular, we were especially interested in testing whether the ideas of MK were reproducible in a differently-formulated model; in this case, a level-model in which mass is not moved somewhat arbitrarily between layers, a process which may have a tendency to produce standing oscillations near the equator. Results are presented in Section 3 using models of increasing realism. In Section 3a a GCM ocean is integrated in a domain exactly the same as in MK with the same resolution and with the same forcing fields to allow a direct comparison with the MK results, while in Section 3b and 3c the full geometry of the Indian Ocean is used. Idealized winds are used in Section 3b and observed stresses in Section 3c.

2. Description of the models used

Two model domains are used in this study. In both, the primitive equations are solved numerically using the model of Cox (1984) based on the finite-differencing method discussed in Bryan (1969), but with the vertical mixing scheme of Pacanowski and Philander (1981). The vertical eddy viscosity is assigned a minimum value of $10 \text{ cm}^2\text{s}^{-1}$ in the upper 10 m of the model to take account of mixing by high frequency winds not present in the model forcing. There are 16 levels in the vertical in a constant depth ocean of 4000 m (see Table 1). The upper 30 m have 10 m resolution. The models differ in the geometry of the domain covered and in the horizontal resolution used.

a. The Somali-region model (SOM experiments)

The Somali region model was used only for idealized integrations. It has a uniform $\frac{1}{3}^\circ$ by $\frac{1}{3}^\circ$ resolution extending from $10\frac{1}{3}\text{S}$ to 25N . The western boundary has an orientation of 45° with respect to the equator (Fig. 2a). The initial stratification is horizontally uniform, with the temperature and salinity values used at each level given in Table 1 and shown in Figure 3a obtained by integrating the Levitus data set over the domain of Figure 3b. A Kelvin wave damper is applied along the eastern boundary by relaxing the temperatures and salinities to these initial values with a

Table 1. Distribution of temperature and salinity used in experiments SOM2 and SOM3, INDB, INDL and INDM. In the case of INDL and INDM, the salinity was 35.000 throughout. The temperature and salinity in SOM2 and SOM3 are as for INDB.

Level	Depth of bottom of box (m)	T(INDB) (°C)	S(INDB) (‰)	T(INDL) (°C)	T(INDM) (°C)
1	10 m	24.681	35.0349	29	28.0
2	20	24.580	35.0663	29	28.0
3	30	24.460	35.0892	29	28.0
4	40.2	24.305	35.1128	29	26.5
5	55.5	24.065	35.1462	29	26.5
6	78.5	23.296	35.1985	29	24.0
7	113	24.411	35.2473	15	15.0
8	165	18.196	35.2464	15	15.0
9	243	15.016	35.2307	15	15.0
10	359	12.604	35.1539	15	15.0
11	535	10.719	35.0225	15	15.0
12	798	8.795	34.9054	15	15.0
13	1193	6.282	34.7982	15	15.0
14	1787	3.840	34.7441	15	15.0
15	2678	2.221	34.7245	15	15.0
16	4000	1.348	34.6971	15	15.0

timescale of a few days. All boundaries are closed in the SOM experiments. The value of horizontal eddy diffusion is $2 \times 10^3 \text{m}^2 \text{s}^{-1}$.

The wind stress fields used in experiments SOM2 and SOM3 are shown in Figures 2a and 2b. The SOM2 wind stress is essentially the same as that used by MK in their equivalent experiment, and represents a Findlater Jet of maximum amplitude 5 dynes cm^{-2} with no background wind stress. The wind stress is simply imposed at time zero and is held constant. Experiment SOM3 has a maximum background wind stress of 1 dyne cm^{-2} (Fig. 2b) imposed in May and maintained through the Summer monsoon (till the end of August), and a Findlater Jet (identical in shape to that of SOM2) of amplitude 4 dynes cm^{-2} imposed during June, July and August (see Fig. 2c). There are no surface heat or salinity fluxes in the SOM model integrations.

b. The Indian Ocean model (IND Experiments)

i. *Idealized integrations.* In addition to experiments SOM2, and SOM3, other 'idealized' experiments were performed using the geometry of the whole Indian Ocean (Fig. 3b) and the wind patches of Figure 4. The geometry is realistic except near Southern Africa and there is fairly good horizontal resolution in the area of interest: the north-south grid spacing is 0.3° at the equator, increasing poleward to a maximum of 1° while the east-west spacing varies from 0.5° in the west, to 1.5° in the

east. The model domain extends from 35E to 125E, and from 35S to 25N. The southern boundary is open, all other boundaries are closed. The meridional part of the horizontal eddy diffusion is high near the southern boundary ($3 \times 10^4 \text{m}^2 \text{s}^{-1}$) decreasing to a constant value of $2 \times 10^3 \text{m}^2 \text{s}^{-1}$ more than 5 gridpoints from the boundary. The zonal part of the horizontal eddy viscosity is $10^4 \text{m}^2 \text{s}^{-1}$ at a resolution of 1.5° , decreasing linearly with the zonal spacing to a minimum of $3.3 \times 10^3 \text{m}^2 \text{s}^{-1}$. The experiments using the whole Indian Ocean geometry are called INDB, INDL and INDM. They differ in the choice of vertical temperature profile used. (See Tables 1 and 2 and Fig. 3a.) The wind forcing consists of a background field (Fig. 4a) and a Findlater patch (Fig. 4b), with the time variation of the forcing as for SOM3. There are no surface heat or salinity fluxes in the INDB, INDL or INDM experiments.

ii. *The seasonal cycle integration.* The geometry and resolution used in the seasonal cycle integration are the same as for INDB, but the surface forcing is different. The surface stresses are the seasonally varying stresses calculated by Hellerman and Rosenstein (1983), while the heat flux is parameterized as:

$$Q = Q_c + \lambda(T_c - T) \quad (1)$$

where Q_c is the climatological net surface heat flux interpolated in time from the monthly-mean values of Esbensen and Kushnir (1981), T_c is the monthly-mean sea surface temperature climatology and T is the temperature of the model surface layer. The solar heat flux is mostly absorbed at the first level, but since the near-surface resolution is so high (10 m), account is taken of the penetration of the solar radiation into the ocean; a "two-band" approximation given by $S/S_0 = R \exp(\eta_1 z) + (1 - R) \exp(\eta_2 z)$ is used, where S is the flux at a depth z , S_0 the surface flux and R , η_1 and η_2 are determined from data for Jerlov optical water type IB (Paulson and Simpson, 1977). The additional term $\lambda(T_c - T)$ is a negative feedback term to constrain the surface temperature. If the heat flux Q_c was 'correct,' the stress correct, the model formulation perfect, and the concept of a seasonal cycle valid, then there would be no need for this term since T would equal T_c . However, there is no other negative feedback in the model (except on the southern boundary), and if, for example, the heat flux Q_c were too high or the model poorly formulated so that the vertical redistribution of heat was inadequate, then surface temperatures could continue to rise or fall. Such climate drift must be checked and the inclusion of the term $\lambda(T_c - T)$ term is one way to do it. Errors in the wind stress climatology can also give rise to an anomalous heat flux as the SST is affected by advection and upwelling, which are related to wind stress. The value used for λ is $35 \text{Wm}^{-2}\text{K}^{-1}$, which corresponds to a damping time of 60 days for a 50 m thick layer.

The precipitation minus evaporation in the seasonal cycle integration is treated in

SOM2 SURFACE WIND STRESS
DYNES/CM²

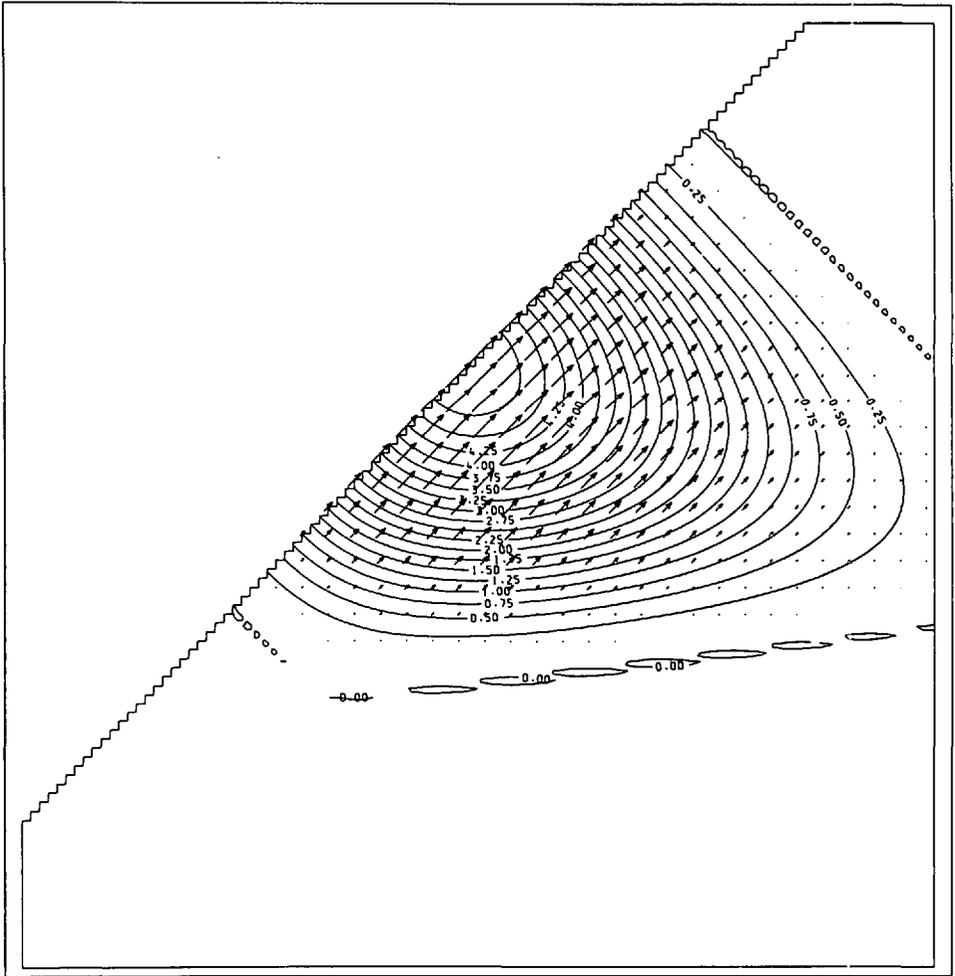


Figure 2. (a) Plot of the Findlater-wind patch used in experiment SOM2 and in the case of SOM3 at 80% of the strength shown. The contour interval is 0.025 Nm^{-2} ; (b) Background wind field used in experiment SOM3; (c) The time evolution of the strength of the wind fields for experiments SOM2 and SOM3.

a similar way to the heat flux:

$$P - E = (P_c - E_c) + \lambda_s(S_c - S)$$

The monthly mean precipitation climatology, P_c , is taken from Jaeger (1976), the climatological salinity S_c is from Levitus (1982), while the evaporation, E_c , is calculated from the Esbensen and Kushnir latent heating. The value of λ_s is taken to

SOM3 BACKGROUND WIND STRESS DYNES/CM2

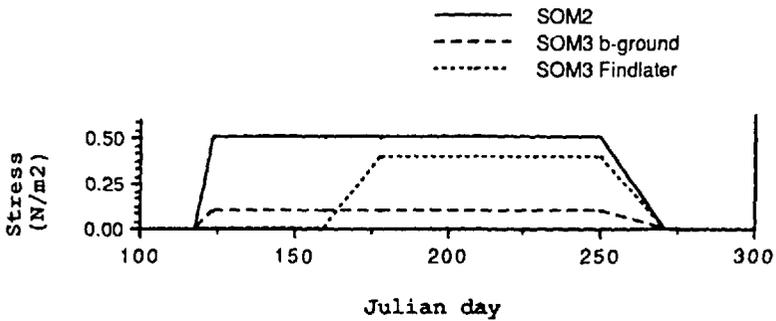
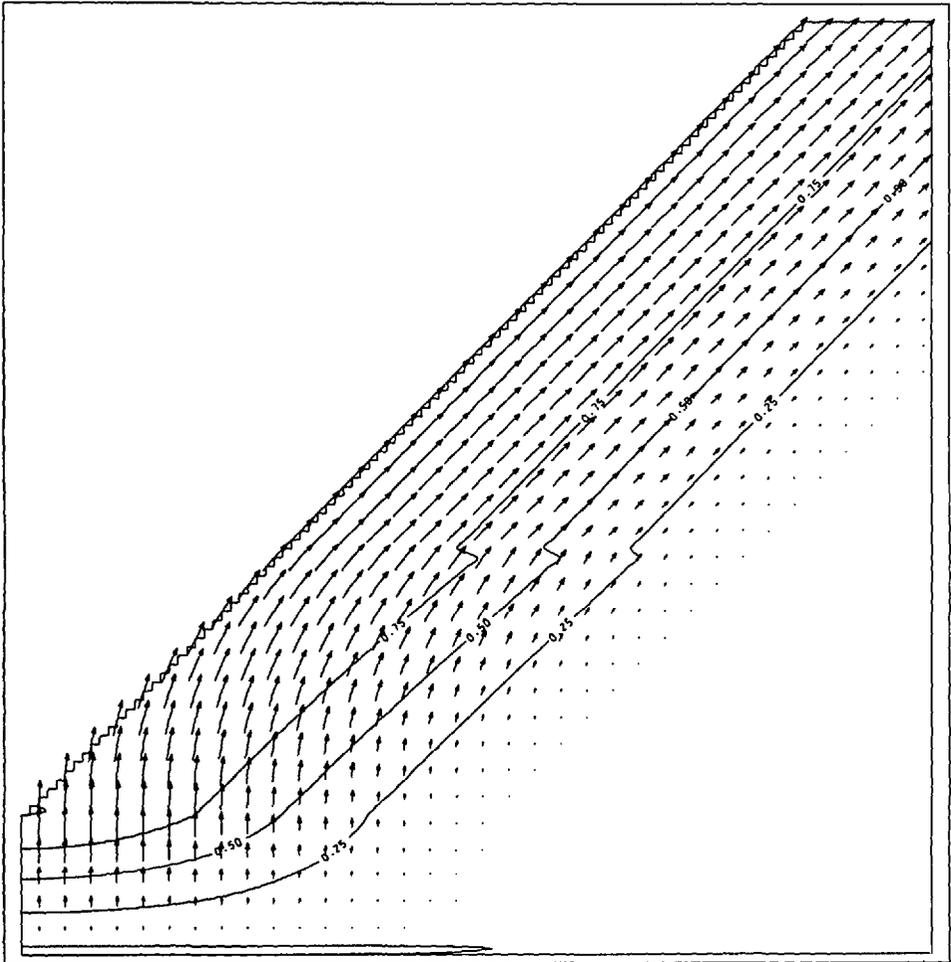


Figure 2. (Continued)

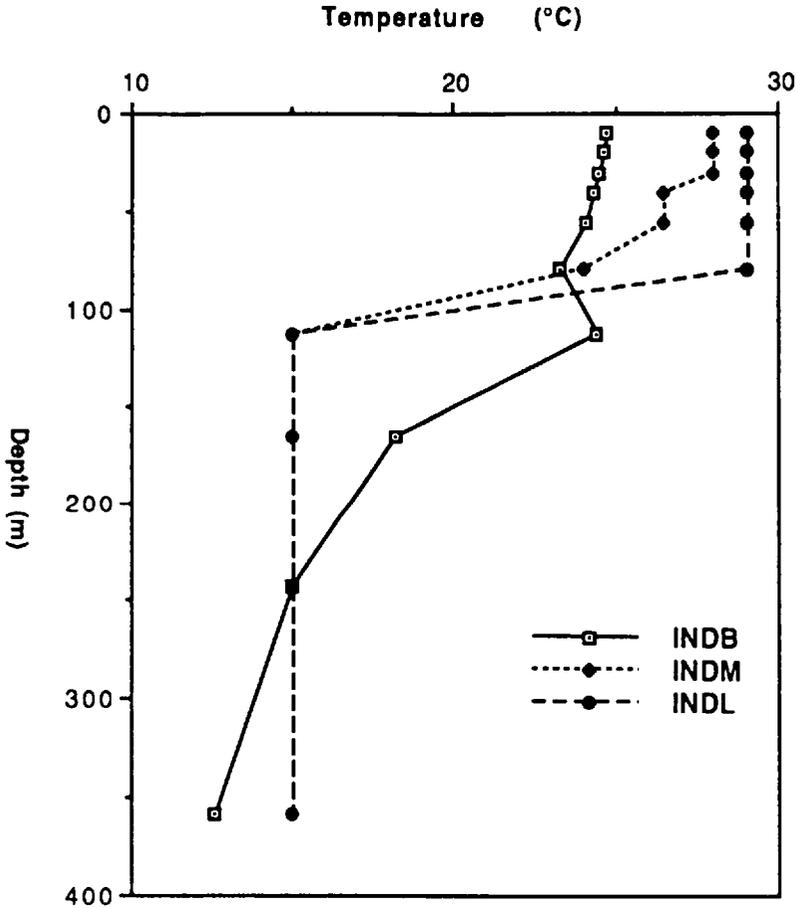


Figure 3. (a) Plot of the thermal structure used in INDB, INDL, INDM. The profile used in INDB is the same as that used in SOM2 and SOM3; (b) Domain of the Indian Ocean used in experiments IND1, INDB, INDL and INDM showing the model resolution.

give the same feedback timescale for salinity as for temperature but there is no physical justification for this feedback. The anomalous heat flux term $\lambda(T_c - T)$ and precipitation minus evaporation term $\lambda_s(S_c - S)$ are of interest since they can point out gross errors in Q_c , S_c , $(P_c - E_c)$ or problems with the ocean model. They are discussed in Carrington (1990), but will not be considered in this paper.

The initial temperature and salinity data for the seasonal cycle integration were the Levitus data for September. The initial velocities were zero, and the calculation started mid-September in a 360-day year. Since the ocean model used in this study has no bottom topography there will be points where there are no Levitus data (i.e. where the ocean model is deeper than the real ocean). In such situations an average value was used based on neighboring Levitus data at the same level. The model was run for three years. The seasonal cycle is taken from the last full year of integration.

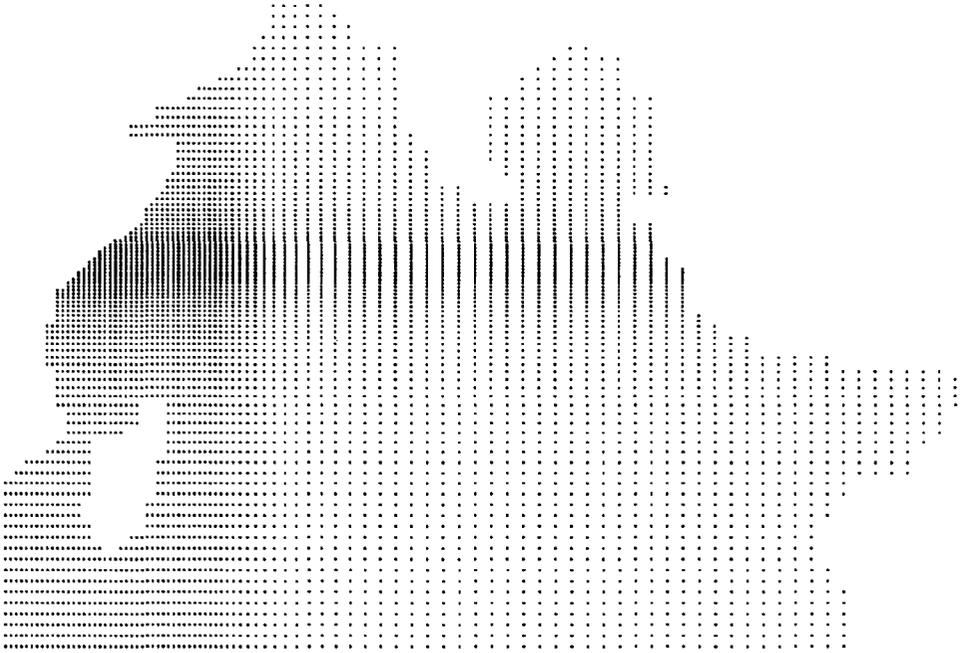


Figure 3. (Continued)

Three years is not sufficiently long to bring the model to full equilibrium, but the surface layers are well adjusted and there are few differences between years 2 and 3 in the region of interest.

3. Results

a. *The idealized Somali Jet wind field experiments (SOM2, SOM3)*

As is true for most experiments to be reported here, the flow in the upper level of the model (5 m) is quite strongly influenced by Ekman drift and for this reason the presence, absence, or movement of eddies is more clearly seen at a level below the surface layer. We will take 35 m as representative of a near-surface velocity. The earlier studies of Cox (1979), Luther and O'Brien (1985), and MK all concentrate on flow in layers 100–300 m thick, but we want to emphasize some of the baroclinic motion between the surface and these depths, so we will not, in general, discuss such strongly-depth-averaged flow.

We consider first, experiment SOM2, the experiment for a Findlater wind-patch, applied to an ocean initially at rest, and maintained for 5 months. In Figures 5(a), (b), (c) we plot the flow at 35 m after one, three, and five months. This experiment was designed to reproduce the results of MK (Fig. 1b), but in fact this does not happen. After one month, the flow is broadly similar to MK in that there is a southern branch to the coastal current which separates at about 7–10N. Subse-

BACKGROUND SURFACE WIND STRESS
DYNES/CM²

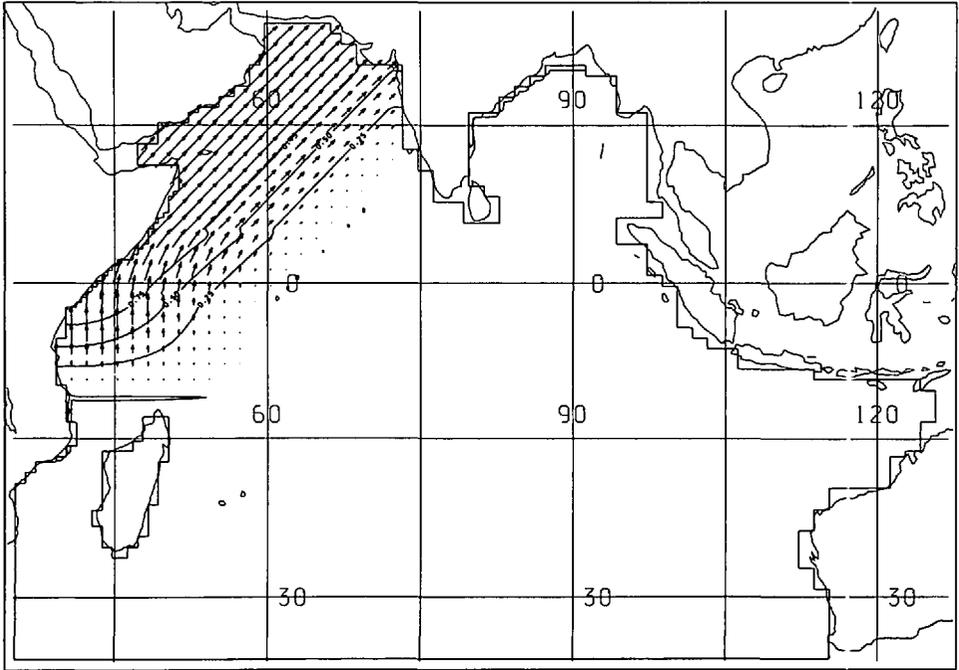


Figure 4. Wind stress used for experiment INDB, INDL and INDM consisting of a background patch (upper panel) and a Findlater jet (lower panel). The time dependence of the wind patches is as for SOM3 in Figure 2c.

quently however the two evolve differently: in MK, there is a northern branch of the current which develops into an eddy and the two eddies then move south and coalesce whereas in Figure 5 the southern branch develops into a strong eddy whose central position does not vary with time (Fig. 5b, 5c).

A strong front is present somewhat to the north of where the boundary current separates from the coast with the thermal front sharper than the current separation which extends over several degrees (Fig. 6). The vertical velocity at 40 m for month 3, given in Figure 7a, shows that there is strong upwelling along the coast from 3N to the separation at 8N and in fact on to at least 15N. This does not have an expression in the surface temperature field south of the separation partly because there is a strong coastal current which advects warm water northward. Beyond the latitude where the jet separates, however, the picture changes and cold water which has upwelled near the coast is advected eastward. There is strong upward motion on the southern edge of the frontal zone, extending to 500 km from the coast.

East of the Great Whirl, a series of jet-like filaments develop: after three months there are two (Fig. 5b); after five months there are three (Fig. 5c). These filaments

IDEALISED FINDLATER JET
WIND STRESS IN DYNES/CM²

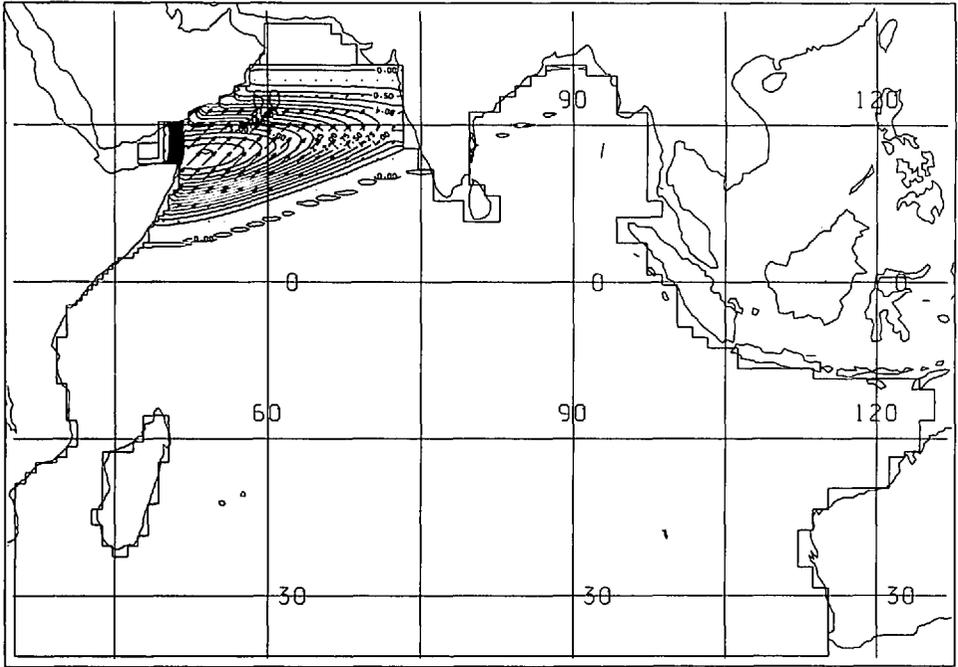


Figure 4. (Continued)

are strong, with currents in excess of 1 m s^{-1} at the surface, and extend progressively farther eastward with time. They may resemble the eddies which occur in the inertial model of Anderson and Moore (1979) but they are not time-independent standing eddies. Although no cut-off eddies form to the north of the main gyre, Figure 5c does show some activity there. The filaments have an SST signature as Figure 6 illustrates,

Table 2. Summary of experiments

- SOM2 High resolution ($\frac{1}{3}^\circ \times \frac{1}{3}^\circ$) model of the Somali region, forced with an idealized wind patch to represent the Findlater jet of maximum amplitude 0.5 Nm^{-2} .
- SOM3 As for SOM2 but with a more realistic wind forcing i.e. with a background wind stress of amplitude 0.1 Nm^{-2} and a Findlater wind patch of structure similar to that of SOM2 but of maximum amplitude 0.4 Nm^{-2} .
- INDB Same geometry as for IND1 but idealized wind forcing is used. No heat flux or P-E forcing. Wind forcing similar (but not identical) to that of SOM3.
- INDL Similar to INDB, but with stratification given in Table 1 and Figure 3a.
- INDM Similar to INDL, but with a slightly different stratification. (See Table 1 and Figure 3a.)
- IND1 Seasonal cycle integration using the full Indian Ocean Geometry forced by climatological momentum, heat and fresh water fluxes, starting from Levitus *T* and *S* data. Run for 3 years with results examined for third year.

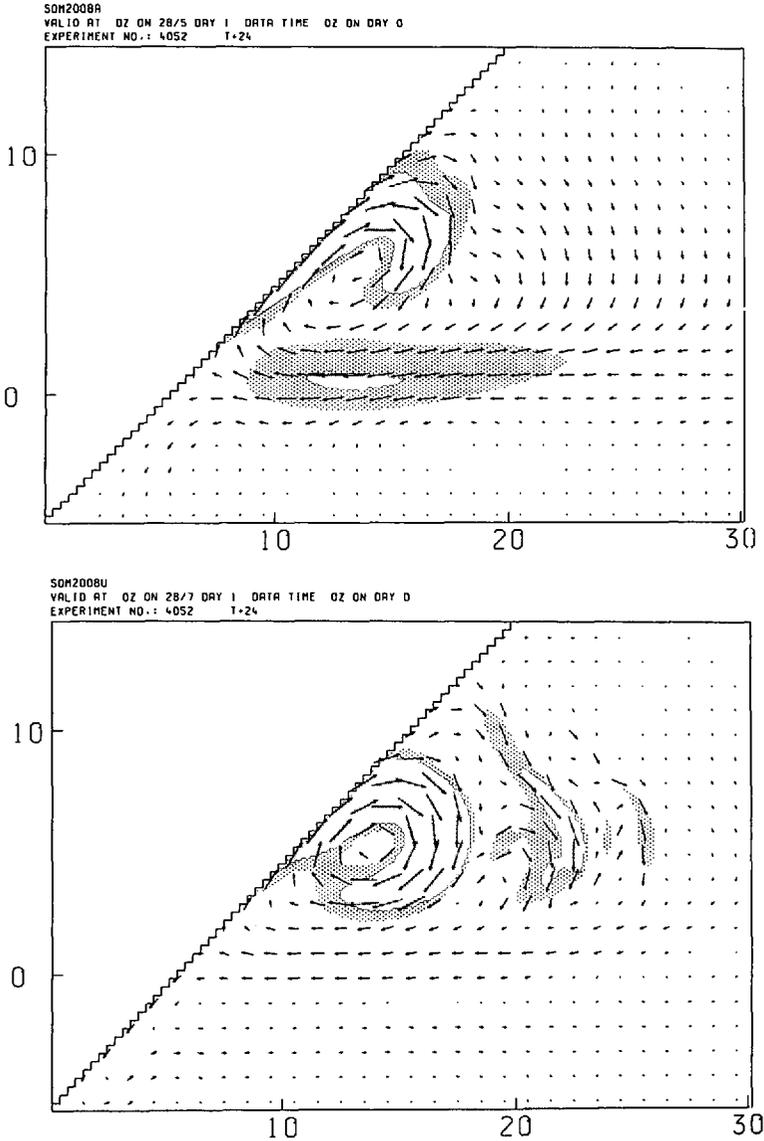


Figure 5. The currents at 35 m for experiment SOM2 after (a) 1 month (end of May) (b) 3 months (end of July) (c) 5 months (end of September). Light shading represents current speeds between 40 cm s^{-1} and 60 cm s^{-1} and heavy shading speeds greater than 60 cm s^{-1} . Only one main gyre develops, although with energetic squirts and jets to the east, northeast.

giving rise to a cusp-like structure where the jets advect cold water from the upwelling region. There is no heat flux in this experiment so there is no damping of the SST field by the atmosphere.

The vertical velocities associated with the filaments are intense. In the vicinity of

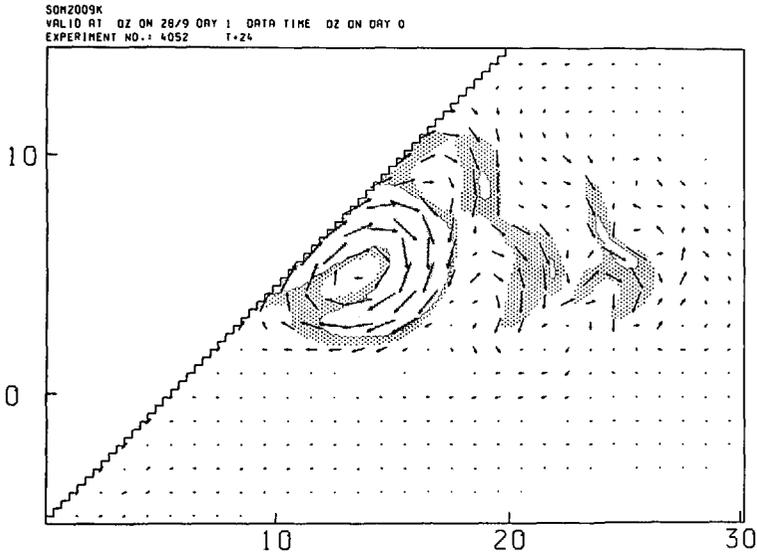


Figure 5. (Continued)

the jets, downwelling is more intense than upwelling (maximum values of order 15 m day^{-1} for downwelling compared to 9 m day^{-1} for upwelling). Cold water sinks along the filaments, though in the main, the axis of strongest vertical velocity is a little to the east of the surface jet. In fact, the axis of cold water lies along the zero of vertical

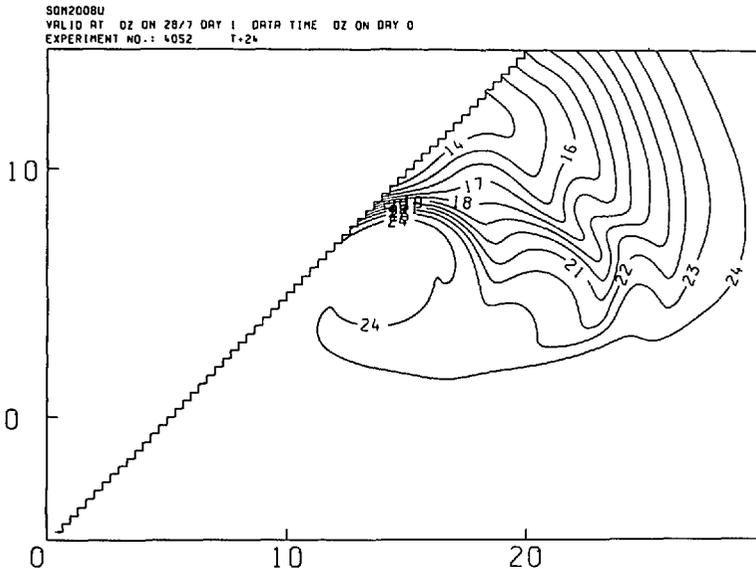


Figure 6. Surface temperature for experiment SOM2 after 3 months, showing the development of a strong front at $\sim 8\text{N}$, to the south of which the temperature gradient is very small.

velocity with sinking of cold water located to the west/southwest of this locus, and upwelling to the east of it. The upwelling does not lead to surface cooling, however, because it is shallower than the thermocline. The sinking motion extends deeper than the upwelling as can be seen on Figure 7b which shows the vertical velocity at 113 m.

The flow at 139 m is shown in Figure 8. Apart from the alongshore flow, the strongest currents are only a few degrees from the equator (2–4N) and are westward. This is consistent with the strong jets of Figure 5 being associated with downward vertical motion. The flow in the upper two hundred meters is of a ‘corkscrew’ type with the flow sinking and spiraling round the gyre, such that the position of the strongest currents rotates clockwise around the gyre with depth. Whereas at 35 m, the strongest flow in the gyre was to the north of the gyre center, at 139 m it is located to the south of the gyre center (excluding the flow immediately along the coast). The gyre extends to depths of c. 250 m. At depths of 300 m the flow is weak and disorganized. Below this, however, the gyre is again evident, much weaker than at the surface, but now rotating in the opposite sense to the surface flow (not shown).

Experiment SOM2 does not confirm the behavior of the equivalent experiment with the MK model but this experiment is not the one which most closely resembles the wind field over the western Indian Ocean. A closer analogue is the wind field used to force experiment SOM3 (which corresponds to Fig. 14 of MK). There is a background wind field, shown in Fig. 2b, together with a ‘Findlater’ wind patch of maximum amplitude 4 dynes which, as in MK, comes on more than a month after the background as shown in Figure 2c. The currents after 1 month, (nominally the end of May), are shown in Figure 9a. There is a strong cross-equatorial coastal flow (up to 80 cms/sec) which separates as a southern gyre, leaving the coast at 3–4N. By the end of June, the strength of the cross-equatorial flow has weakened even though the cross-equatorial wind has not changed, by the end of July it is only $\sim 20\text{--}30\text{ cm s}^{-1}$ and at the end of August slightly weaker still (Fig. 9b). Meanwhile the Great Whirl spins up following the onset of the Findlater wind patch and becomes the major feature.

The low-latitude separation $\sim 3\text{N}$ which is most evident in May, before the onset of the Findlater patch, may be a result of Ekman flow which, in response to a southerly wind, will be to the east in the northern hemisphere and to the west in the southern hemisphere, with nonlinearity acting, via conservation of potential vorticity to strengthen the eastward and weaken the westward flow (Cane, 1979; Philander and Delecluse, 1983). The separation continues to exist through August but has largely gone by the end of September following the turn-off of the winds. It is not associated with a thermal front at any stage. A strong front is present, but only to the north of the Great Whirl. The SST pattern is shown in Figure 11c for July. The front to the north is not wedge-like because there is no onshore flow to the north of the Great Whirl (i.e. there is no Socotra Eddy) and there is no wedge to the south of the Great Whirl. There is some sign of a wedge while the southern flow is developing and

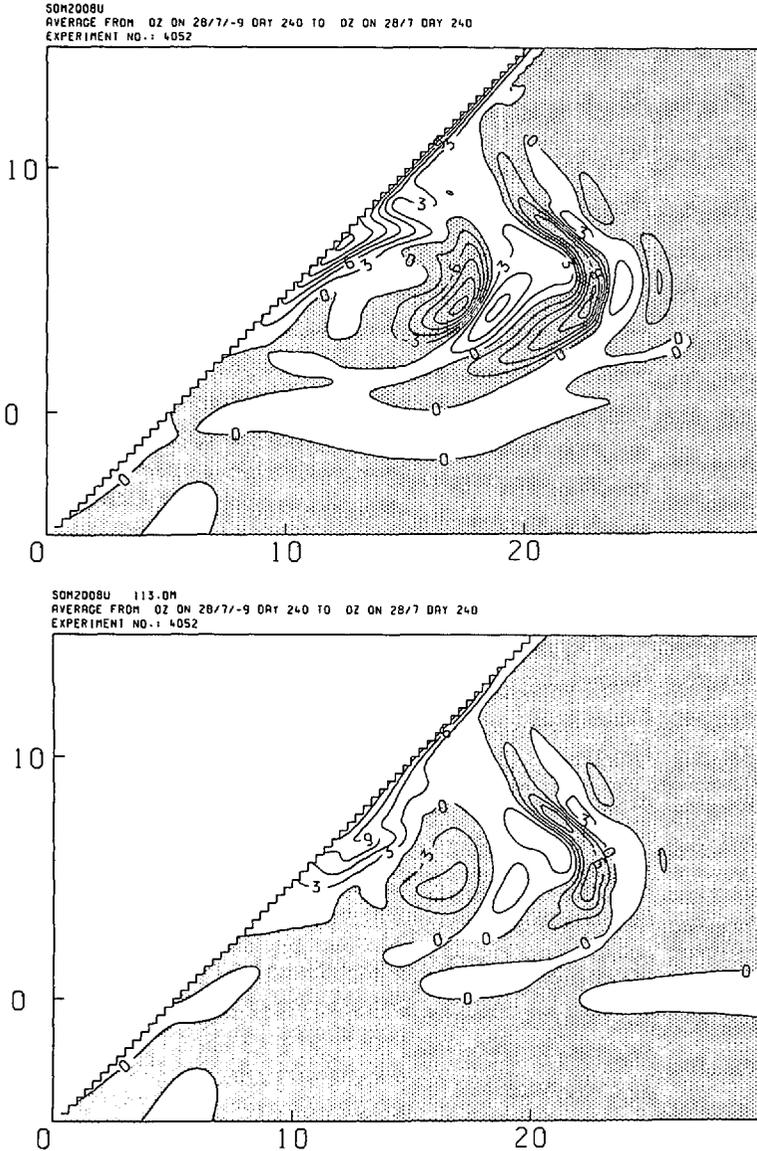


Figure 7. Vertical velocity at (a) 40 m and (b) 113 m for experiment SOM2 after 3 months. Units are meters/day. Shading represents downward motion. There is strong upwelling along the east, even south of 8N, but this upwelling does not lead to cold SSTs. There are strong vertical circulations associated with the squirts and jets of Figure 5.

has a strong turn off, but as time evolves, this turn-off weakens and the front quickly migrates north. The lack of frontal structure will be considered further in Section 3b.

Some features of the GCM results are similar to those in the MK layer model, others not. The broad-scale pattern is rather similar to that of MK but the small-scale features are quite different. For experiment SOM2, the Great Whirl spins-up in the

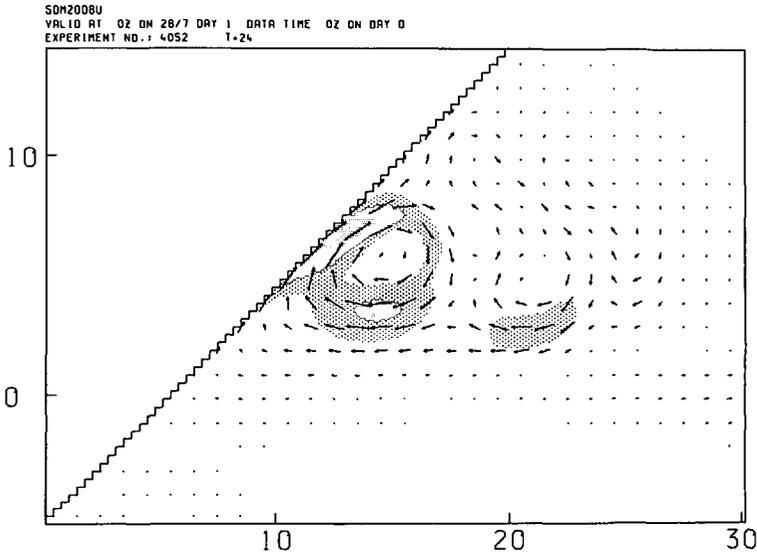


Figure 8. Currents at 139 m for experiment SOM2 after 3 months. Shading is as for Figure 5. At this depth the region of strongest currents, excluding the boundary current, is on the southern side of the gyre, in contrast to Figure 5 when it is on the north of the gyre near the surface.

early stages (Fig. 5a) rather as in MK. However, as time evolves, this gyre develops jet filaments to the east, but no strong secondary gyres form to the north. (There is a weak feature to the North of the Great Whirl but no onshore flow there.) Why the eddy dynamics of the GCM are different to those of the layer model is not clear. One possibility is that baroclinic instability processes are different. An analysis of the energetics of the layer model carried out by McCreary (private communication) shows that there is an additional source of baroclinic energy arising from temperature as well as depth variations within a layer. A second possibility is that frictional effects are different. The horizontal resolution is the same in both models and although the value of horizontal mixing of momentum is the same, that of heat is lower in the GCM than in the layer model ($2 \times 10^3 \text{m}^2/\text{s}$ in the GCM compared with $5 \times 10^3 \text{m}^2/\text{s}$ in MK). There are differences in the form of vertical mixing of both momentum and heat however. In the layer model there is no explicit mixing.

To test if the different dynamics resulted in some way from different vertical mixing, experiment SOM3 was repeated with the explicit vertical mixing in the upper ocean reduced, but with the wind applied in a layer. The wind was applied in a layer 96 m deep (comparable to the depth of the mixed layer in the MK model near the Somali gyre). The results (not shown) are not qualitatively different from those of SOM3. In particular there is no evidence of vacillation, no cold wedge on the north of the low-latitude turn-off and the structures of the offshore flow patterns are very similar to those of SOM3. Why the MK model produces two eddies along the coast

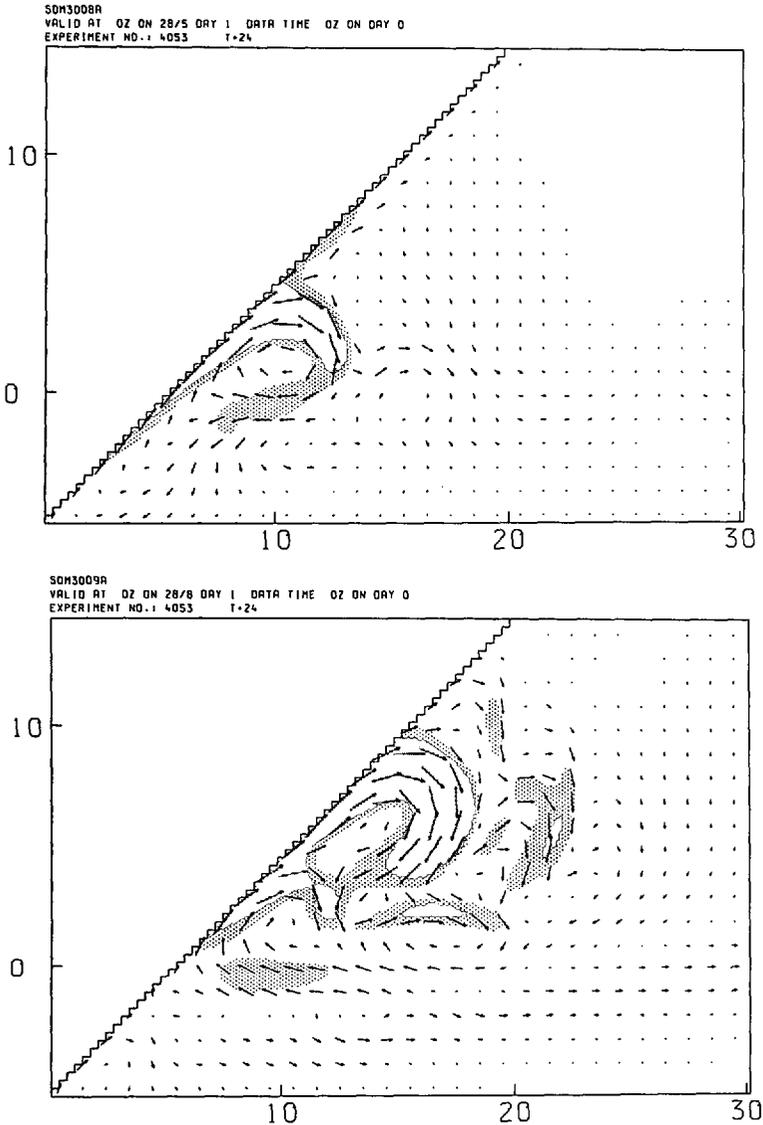


Figure 9. Currents at 35 m for experiment SOM3 at the end of (a) May (b) August, showing the development of a double separation from the coast. The southern one is not associated with cold water at the surface.

which then interact and exhibit interesting longshore movements, whereas the GCM produces only stationary features is not clear. Nor is it clear why the GCM does not produce a southern cold wedge but this will be considered in the next section.

There are features of agreement however. The cold water wedge to the north of the Great Whirl is present in both models, and in both there is upwelling along the

coast, between the equator and approximately 4N which has no signature in the SST. This lack of an SST signature is partly a result of the horizontal advection of warm water from the south but in the GCM partly a result of the vertical temperature distribution, in that, south of 8N, upwelling does not extend below the thermocline and cold water is not brought to the surface whereas coastal upwelling north of 8N is quite strong and extends deeper than at lower latitudes, so bringing cold water to the surface.

b. Results from the IND experiments using simulated winds

It has been demonstrated by Cox (1979) and by MK that the details of the Western Boundary flow can be sensitive to the geometry used in the model. This suggests that we should perform integrations in a geometry more like that of the Somali basin. The model is as described in 2b. It covers the whole Indian Ocean, with the variable resolution shown in Figure 3 but only the Somali Current—Arabian Sea region will be discussed below. As in Section 3a, idealized winds are used: the background wind and the wind patch are shown in Figures 4a,b respectively, with the time evolution as for SOM3. The wind patch is not quite the same as used in MK or in SOM3, but is perhaps slightly more realistic, in that the axis of strong winds lies slightly to the northeast rather than to the southeast. Three experiments are described which differ in their initial thermal structure. The first of these to be discussed, INDB, uses the same stratification as for SOM2 and SOM3.

At the end of May (30 days into the integration) there is a strong separation from the coastline at about 3N at the surface (Fig. 10a). North of this southern separation, the flow is weak because the 'Findlater Jet' has not yet turned on. As the Findlater Jet strengthens, the Great Whirl spins up and can be clearly seen in Figure 10b for August. The center of the gyre moves slightly northward between July (not shown) and August. During September, the winds die away. The Great Whirl continues to move slowly northward during September but the center is only one degree farther north than at the end of August. The southern cross-equatorial flow dies away rapidly as the wind is turned off, but even in August when the winds are at full strength, the cross-equatorial currents have reduced to 30 cms/s compared with 60 cms/s in May. As in SOM3 the cross-equatorial flow is quite shallow and extends only to about 100 m, whereas the Great Whirl can be weakly seen at 666 m in August (not shown). At all depths the southern gyre and the Great Whirl are separate. There is no cold wedge between the gyres (Fig. 11a).

What features of the flow resemble those of SOM3? First, in both cases, there is a cross-equatorial flow which separates from the coast at about 3N and a deep gyre forms to resemble the Great Whirl. Secondly, the strength of the cross-equatorial flow weakens with time even though the cross-equatorial winds do not, and the depth of the cross-equatorial flow is shallow (100 m). The behavior in experiment INDB appears to differ from that of SOM3 in that the southern separation remains more

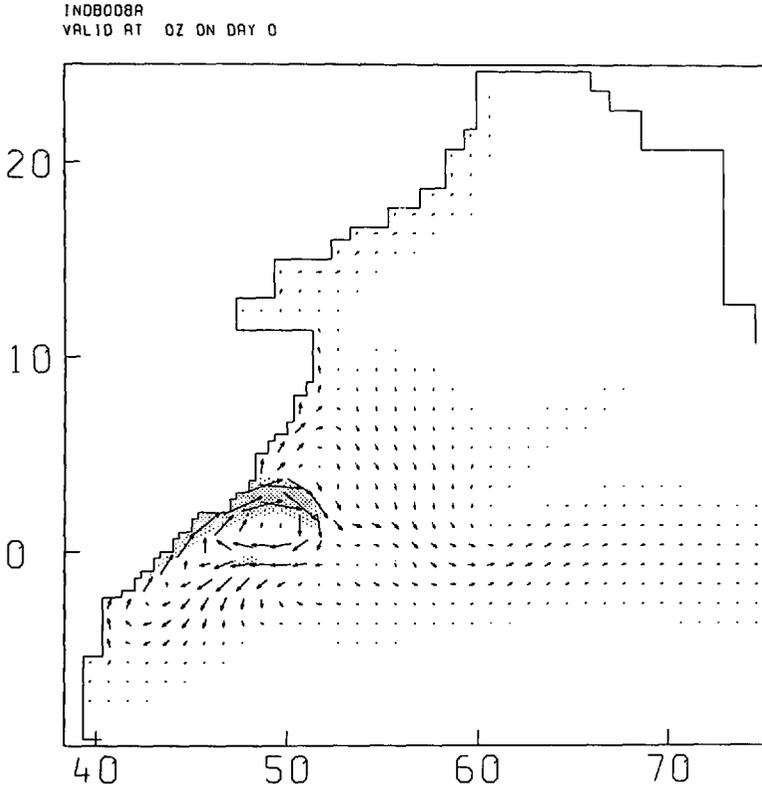


Figure 10. Currents from experiment INDB at (a) 35 m for May, (b) 35 m for August, showing that the two gyres are well separated and do not interact, and (c) 139 m for August, showing that the low latitudes gyre is shallow. Shading is as for Figure 5.

distinct from the Great Whirl which is located farther north with no eddy structure to the east. In neither case does the southern separation propagate northward to merge with the Great Whirl and there is no cold wedge at the northern edge of the southern separation. The cold wedge is a strong feature of the MK model and in the observations. Why does it not occur in the GCM results? One possibility is that upwelling does not extend deep enough or that the subsurface thermal structure is not correct. In Figure 3a the thermal structure used in INDB is shown together with the much sharper temperature profile used by MK. If there were upwelling of subsurface water from below 75 m, in the MK model this water would be cold while in the present experiment it is not. Could this influence the low-latitude separation? To test this, two further experiments were performed, (INDL and INDM) which used the stratification given in Table 1 and shown in Figure 3a.

The changes in stratification between INDL and INDM seem quite modest, but do have a noticeable influence on the SST pattern and flow field. Although the thermal profile of INDL more closely resembles that used by MK, it does not result in a

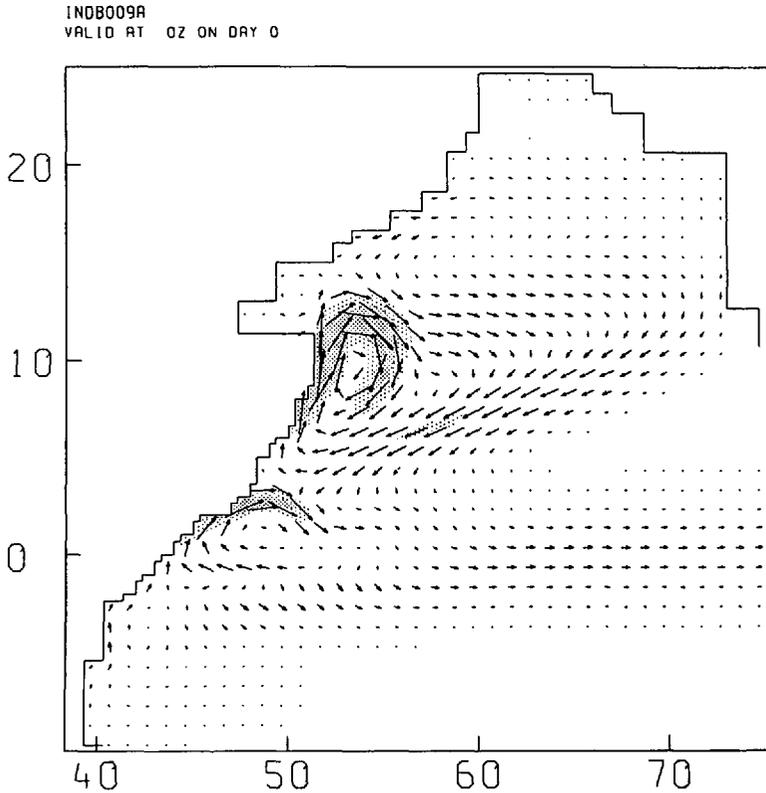


Figure 10. (Continued)

low-latitude cold wedge. Experiment INDM, however, does produce a cold wedge. In May there is just a single cold wedge, most pronounced at and north of the southern separation. By June a second cold wedge is beginning to form at a higher latitude and by July is quite well developed (Fig. 11b). In August (not shown) the cusp-like behavior to the north of the Great Whirl seen earlier in Figure 6 is evident. By contrast, in experiment INDL, the southern cold wedge while present in June, has gone by July (not shown).

In addition to influencing the thermal pattern at the surface, the change in thermal structure also changes the flow field. This can be seen in Figure 12a,b which shows the 35 m currents for Aug for (a) INDL and (b) INDM. The southern separation is much more pronounced in INDM than in INDB. Figure 12a should also be compared with Figure 10b. The southern separation is well-defined in the flow field of Figure 10b (though not in the surface temperature shown in Figure 11a) but the Great Whirl is much farther north, so the two gyres are well separated and do not interact. In the case of INDM, the Great Whirl is several degrees farther south, allowing more interaction between the gyres. The southern separation is well-defined in the velocity field of INDM and INDB but not in the case of INDL. There is

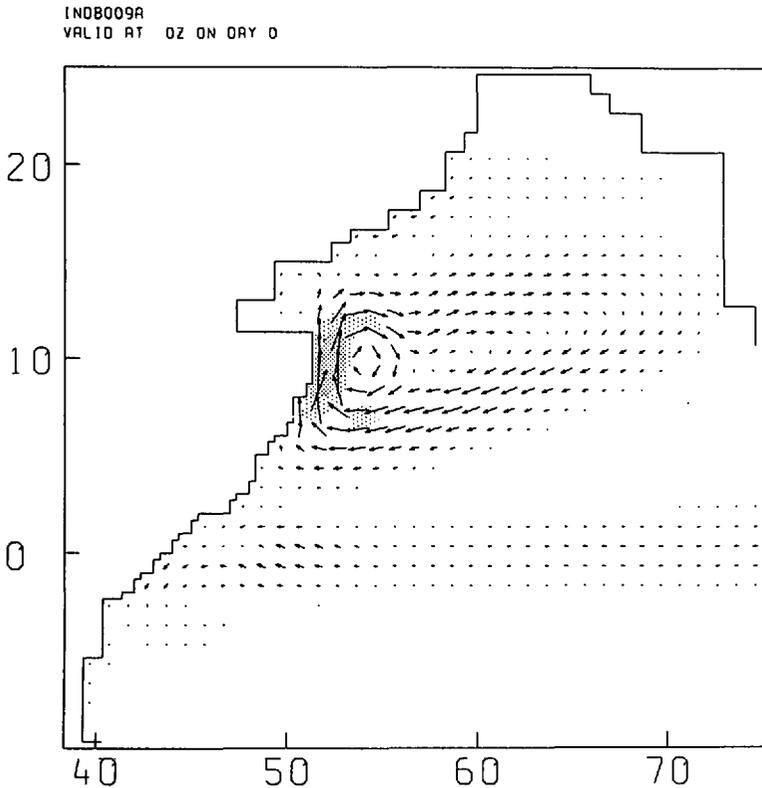


Figure 10. (Continued)

further gyre activity to the east of the main gyre in INDL and INDM, absent in INDB.

The conclusion from these experiments is that the difference in the geometry between the SOM and IND experiments does not lead to major changes in the response; two gyres still develop, a cold wedge forms on the northern edge of the Great Whirl but not on the southern gyre and the two gyres do not interact strongly.

The results are sensitive to the thermal stratification, however. When this is changed slightly as in INDM, two significant improvements result. A cold wedge forms to the north of the southern gyre and the position of the Great Whirl is located farther to the south. In this respect the GCM more closely resembles the MK results and the observations but significant differences still remain in the GCM: energetic structures are produced to the east and slightly to the north of the Great Whirl, but the Socotra Eddy develops and the southern 'gyre' does not migrate north to merge with the Great Whirl. Such a migration is evident in the observations, but it is not clear if this is associated with changes in the wind. Schott (1983) argues not, since in at least two of the three cases he analyzed, he noted no obvious changes in the wind as the gyre migrated north. The GCM results using idealized winds therefore appear

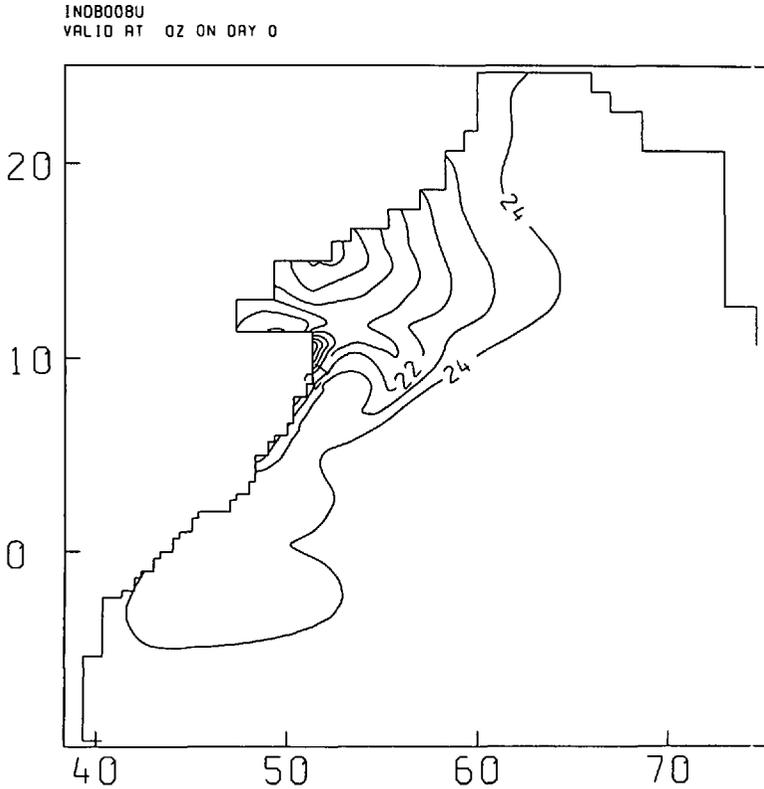


Figure 11. Surface temperature for July for (a) INDB, (b) INDM and (c) SOM3 showing the presence of a southern cold wedge only in INDM.

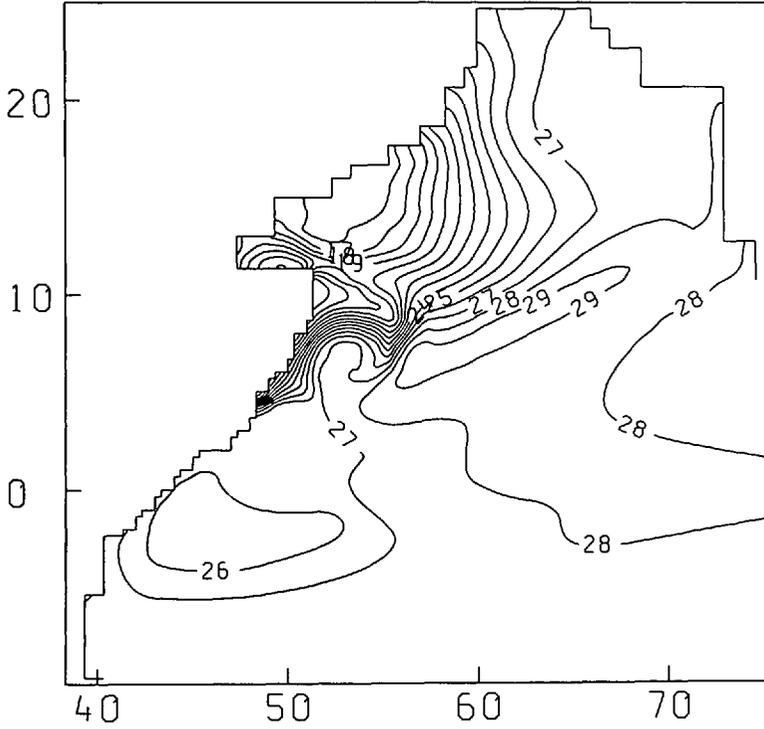
to be at variance with the observations in this respect. None-the-less the overall pattern of flow in Figure 12b is very similar to that of Figure 1. Gyres A, C, D and the weaker gyre to the east of D are all well simulated. The major discrepancy is the absence of the Socotra eddy (B). It may be necessary to include the island of Socotra to obtain a good simulation of this gyre.

While the results of Section 3a and 3b show that the southern gyre develops rapidly in response to the longshore wind, Southern Hemisphere mean winds might none-the-less influence its development even though they are not necessary to produce it. Likewise the occurrence of the southward flowing coastal current just before the southwesterly longshore winds turn on in May may also influence the development of the southern gyre. To test the model response to more realistic winds, the model was run through a seasonal cycle using Hellerman and Rosenstein (1983) winds. This is discussed in the next section.

c. Results from the seasonal cycle integration INDI

An annual cycle integration using the full geometry of the Indian Ocean (Fig. 3) was carried out, though only the western part is considered here. Figure 13 shows the

INDH008U
VALID AT 0Z ON DAY 0



SOM3008U
VALID AT 0Z ON 28/7 DRY 1 DATA TIME 0Z ON DAY 0
EXPERIMENT NO.: 4053 1-24

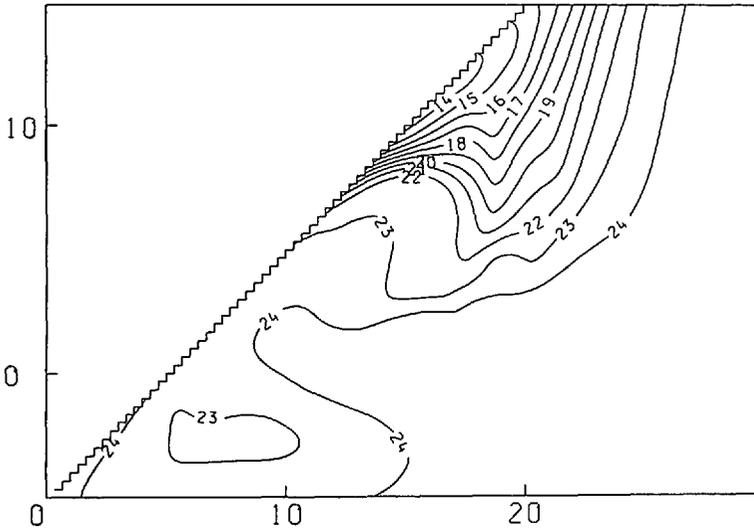


Figure 11. (Continued)

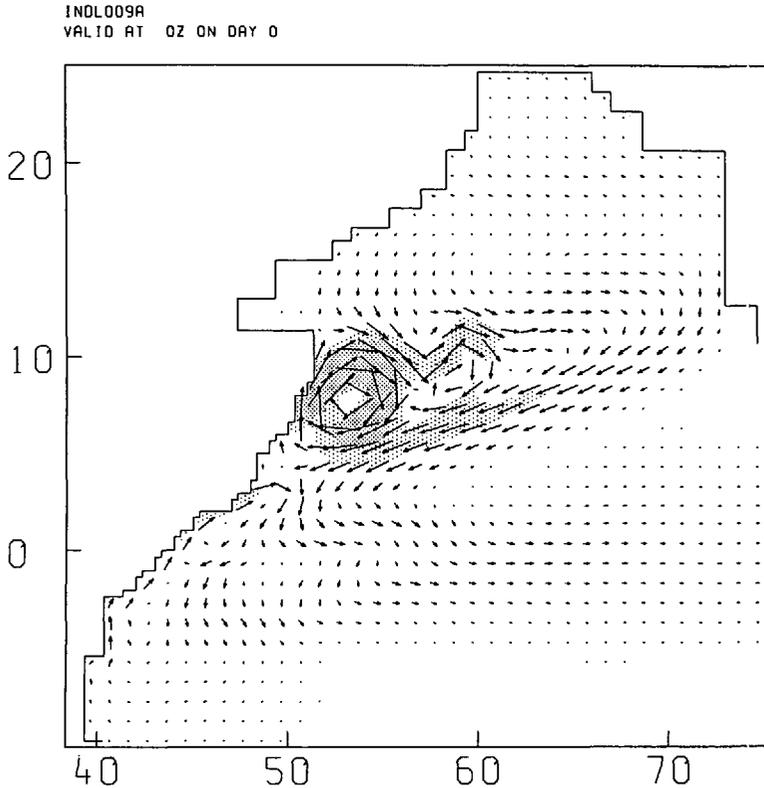


Figure 12. Currents at 35 m for the end of August for experiment (a) INDL and (b) INDM.

currents at 35 m depth for selected months throughout the 3rd year of integration. We will begin discussing Figure 13 toward the end of the NE monsoon. In April, the flow is southward from about 3N to a meeting with the East African Coastal Current (EACC) at 5S. North of 5N the flow is to the north. Both currents are fed by westward surface flow at about 4N which splits, when it reaches the coast, into a northward and a southward branch. The flow in the Great Whirl region is therefore northward long before the Findlater jet sets in. In fact there is weak northward flow there even in January of strength 10 cm s^{-1} , with the main branch of the southwestward Somali Current lying nearer the equator.

Returning to the April situation, the northward-flowing East African Coastal Current (EACC) and the southward-flowing (but weakening) cross-equatorial flow meet at about 5S and form a broad eastward flow which extends over much of the basin, and merges into the Wyrтки jet (Wyrтки, 1973) along the equator farther to the east. The southward cross-equatorial flow however is shallow. The northward flowing branch of the Somali Current (at $\sim 7\text{N}$) extends to about 100 m. There is no sign of a remnant Great Whirl from the previous southwest monsoon as has been suggested by Bruce and Volkmann (1969).

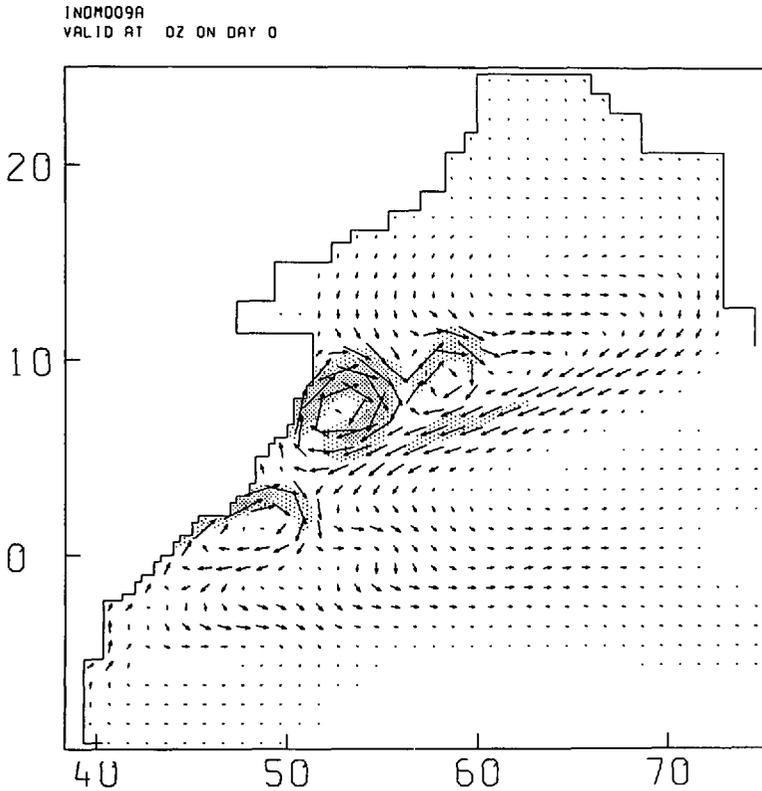


Figure 12. (Continued)

By May the flow in the EACC at 35 m has extended northward to the equator to a turn off at 1–2N. This flow appears to be distinct from that in the Somali Current farther north which at this time is maximum at about 7N. In June a Great Whirl is building, but the center is still quite far south at 6N. The cross-equatorial flow is stronger and seems to be less distinct from the Great Whirl than was the case in May. The Great Whirl is still quite shallow, extending to only about 100 m depth.

At the height of the monsoon in July (see Fig. 14) the cross-equatorial flow continues into the Great Whirl, still centered at about 7N. There is evidence for offshore flow in the cross-equatorial jet at 67 m, but at greater depths (139 m) this separation is less clear. The Great Whirl itself has an interesting vertical structure which can be seen in the current structure at 35 m, 48 m and 96 m (Fig. 14a,b,c). Like the idealized SOM calculations, there is a corkscrew appearance to the gyre; the alongshore flow leaves the coast at 35 m and an eastward flow on the northern edge of the Whirl is evident. At 48 m, this eastward flow is much less apparent, but a southward flow on the eastern edge of the Whirl is evident, while at 96 m one sees westward flow on the southern edge of the Whirl. The flow along the coast is northeastward throughout.

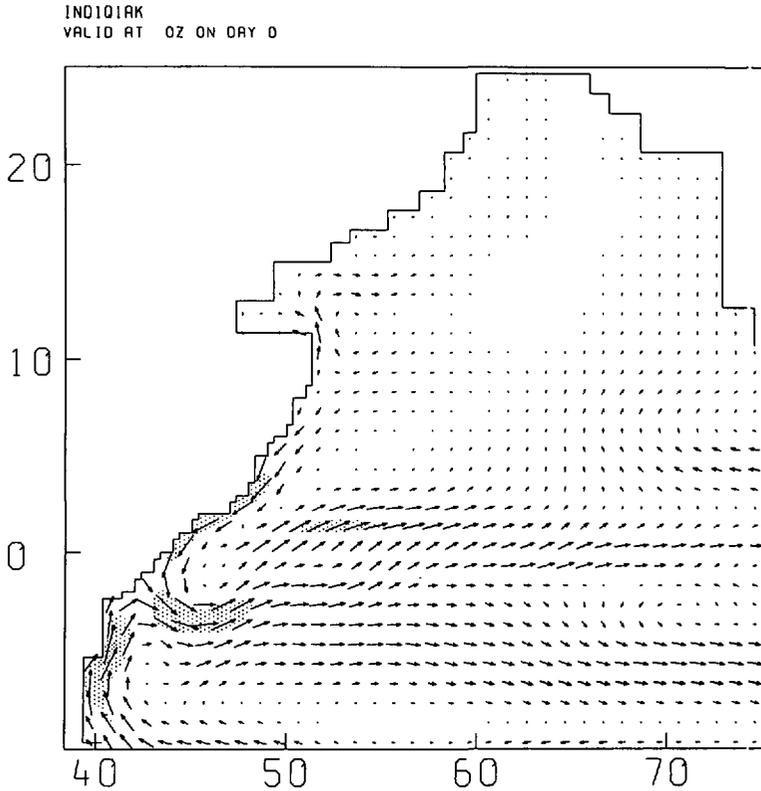


Figure 13. Currents at 35 m from experiment IND1 for (a) Dec, (b) Feb, (c) April, (d) June, (e) Aug, (f) Oct. Shading is as for Figure 5. There is northward flow along the Somali coast in January, (in a direction opposite to the wind which has a component to the south during the N.E. monsoon). This current is a remnant of the Great Whirl. The currents in June show a more complex structure than has been observed with 3 separations, which is maintained through August. The southern separations are not marked by cold water wedges in SST (not shown).

The gyre continues to strengthen into August and to extend deeper to depths of about 200 m. A corkscrew type behavior is still present (not shown). The cross-equatorial flow does show weak separation at about 4N at the 35 m level but can be more clearly seen at 96 m. (This is not shown for August but can be seen in Fig. 14c for July.) The center of the Great Whirl is still at about 7N although its zone of influence has expanded to the north (Fig. 13d). Figure 13d and e show that the current separations are quite complicated with three separations: one near the equator, one at 3–4N and one at ~8N.

Between August and September the Great Whirl changes from being quasi-circular to more elongated, the zone of weak currents which marks the center moving to 10N. There is a corresponding northward shift in the latitude of eastward currents denoting the northern extent of the gyre. At 200 m the center is more clearly defined

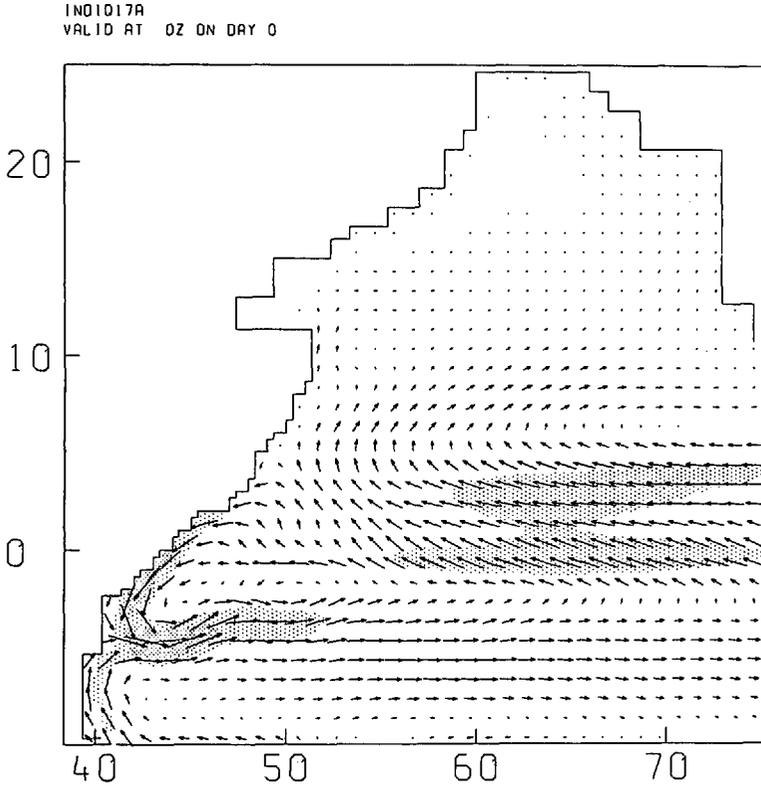


Figure 13. (Continued)

at 11N, and at greater depths it is even farther north. There is some sign of the system reverting to a two-gyre structure in September with a southern separation at about 3N beginning to reform, consistent with the observations of Schott (1983). In October the Great Whirl has moved even farther to the north. It can still be seen at 200 m in October, but by November there is little evidence for it at this depth. There is northward flow at about 11–12N at the coast at depths to 100 m, but it is difficult to call this an eddy. This flow is still present in December but from the December plots alone it is not possible to find the origin of this northward flow. The time sequence shows that it is the last vestige of the Great Whirl formed five months earlier farther to the south.

Farther south, the flow is to the southwest under the influence of the northeast monsoon (in November beneath the surface flow there was already weak flow to the southwest, but it is not until December that this is clearly visible at the surface). The flow to the southwest is confined to depths shallower than 66 m in the model. In January the near-surface flow across the equator is from the northeast pushing the northern extent of the EACC southward.

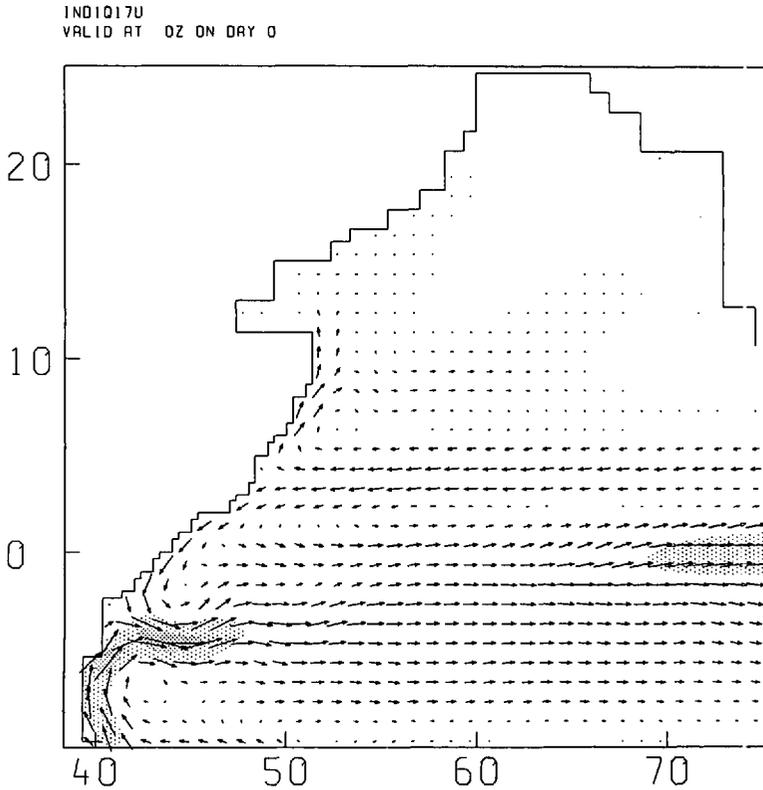


Figure 13. (Continued)

4. Summary and conclusions

In this paper we have considered some of the factors to which the flow along the Somali coast is sensitive. A model using the same geometry (see Fig. 2) and resolution as MK (McCreary and Kundu, 1988), but with 16 levels in the vertical as opposed to two layers, was integrated for several months using wind profiles similar to those of MK. Two experiments were reported, SOM2 and SOM3, which differed in the form of the wind profile used. In SOM2, there was a wind stress of maximum amplitude 0.5 Nm^{-2} representing the Findlater jet, while in SOM3, there was a background wind stress of 0.1 Nm^{-2} together with a Findlater jet of 0.4 Nm^{-2} . In both, a Great Whirl formed in response to the Findlater jet, with cold water on the northern edge. In SOM3, there was initially a cross-equatorial flow, in response to the cross-equatorial winds, which separated a few degrees north of the equator. This current was always shallow ($\sim 100 \text{ m}$), developed quickly following the onset of the winds but subsequently weakened even though the winds did not. At no stage was there a cold wedge between this southern flow and the Great Whirl as there was in the MK model. The Great Whirl exhibited a corkscrew motion in the vertical and

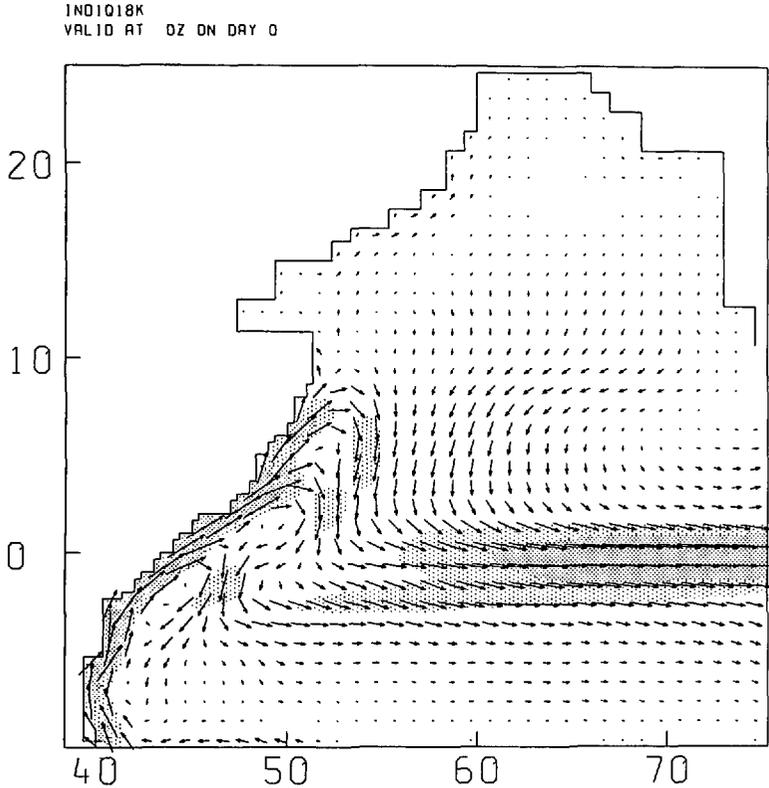


Figure 13. (Continued)

cusps associated with squirts and jets developed to the east (more pronounced in SOM2). In the MK model, the southern separation moved northward as the low-latitude gyre interacted with the Great Whirl, even though there was no change in the winds. In the GCM model, the southern separation remained fixed and did not move northward. MK argued that there was strong nonlinear interaction between the southern flow and the Great Whirl giving rise to vacillation. No such vacillation was exhibited by expt. SOM3 (or any other of our experiments).

INDB was an experiment using idealized winds, similar to those of SOM2 and SOM3 but perhaps a little more realistic and using the full geometry of the Indian Ocean. As in SOM3, a shallow cross-equatorial flow developed rapidly in response to the background wind, but subsequently the strength of this flow decreased with time. In response to the Findlater jet, a deep Great Whirl developed which again exhibited a corkscrew behavior. A cold wedge formed on the northern edge of this gyre, but there was no cold wedge to the south of it: throughout the whole integration the cross-equatorial flow remained distinct from the Great Whirl which was located farther north than in SOM3. Two other experiments were performed, in which the

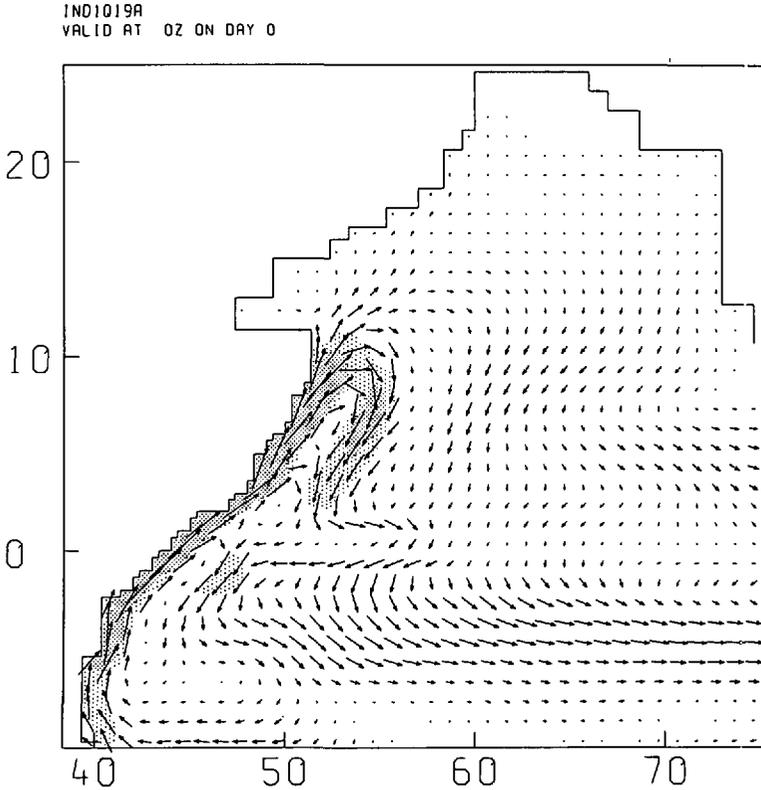


Figure 13. (Continued)

stratification was modified. In INDL, in which the same temperature profile as MK was used there was again no southern cold wedge, but there was in INDM in which a slightly shallower thermocline was used, suggesting that the formation of the wedge is sensitive to the vertical stratification. Although there was coastal upwelling in INDB, INDL and INDM it was only in INDM that this upwelling brought sufficiently cold water to the surface. A notable feature of INDM was that the Great Whirl was located several degrees nearer to the equator than in INDB. The southern cold wedge did not move north as a result of self interaction between the gyres as in the MK model, however, and no vacillation resulted.

There are significant differences between the low-latitude vertical structure of the model and that observed. Swallow *et al.* (1983) noted during Index 1979, that the current shear in the vicinity of 2–3N in June was very strong: surface currents were between 3 and 4 ms^{-1} , while at 50 m were more like 0.5 to 2 m s^{-1} . There was a strong density gradient throughout the upper 100 m. The Richardson numbers were significantly below 0.25 in the upper 50 m. Model results have shown that the dynamics are quite sensitive to the vertical stratification suggesting that the vertical

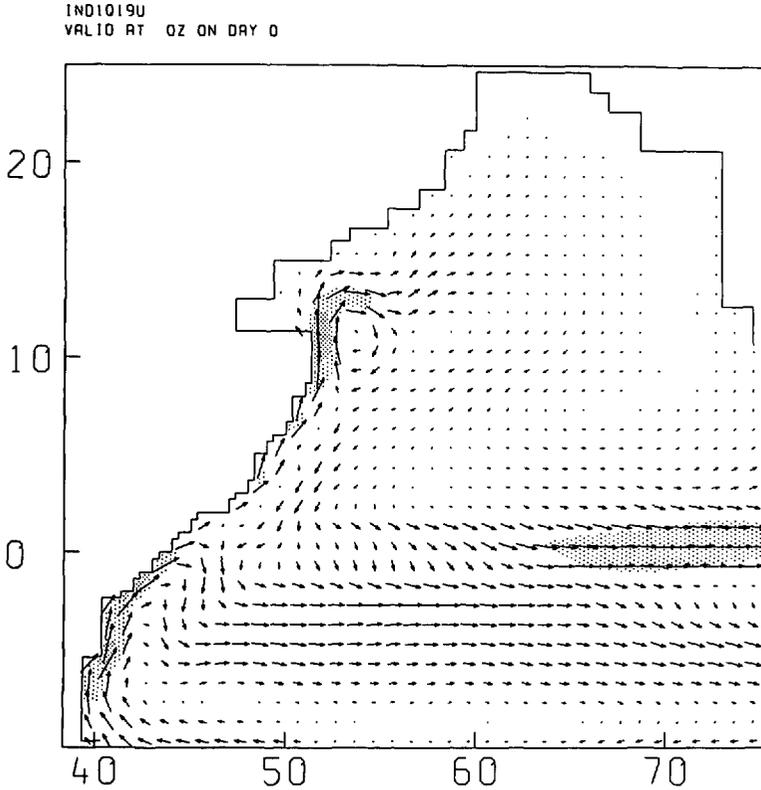


Figure 13. (Continued)

mixing in the GCM may be inadequate. Certainly model currents and shears appear to be much smaller than those observed.

Experiment IND1 was a seasonal cycle integration using the full geometry of the Indian Ocean started from the Levitus data for September and carried forward for 3 years forced by Hellerman and Rosenstein wind stresses. Although the integration was for the whole Indian Ocean only the seasonal cycle of currents in the vicinity of the western boundary was examined in this paper. The Somali Current flows northward in the very northern part of the Somali coast, as early as January and long before the winds there are northeastward. This flow in fact appears to be a remnant of the Great Whirl of the previous summer. Farther south the flow is to the southwest to a convergence with the East African current at 5S. As the N-E winds weaken, the extent of the East African current moves north until it crosses the equator and separates at a low latitude in May. Later in the S-W monsoon season, this flow merges with the Great Whirl. There is still a partial separation from the coast but it is not as pronounced as in the idealized experiments. In fact there are two low latitude separations; one near the equator and one near 4N but there is no strong indication

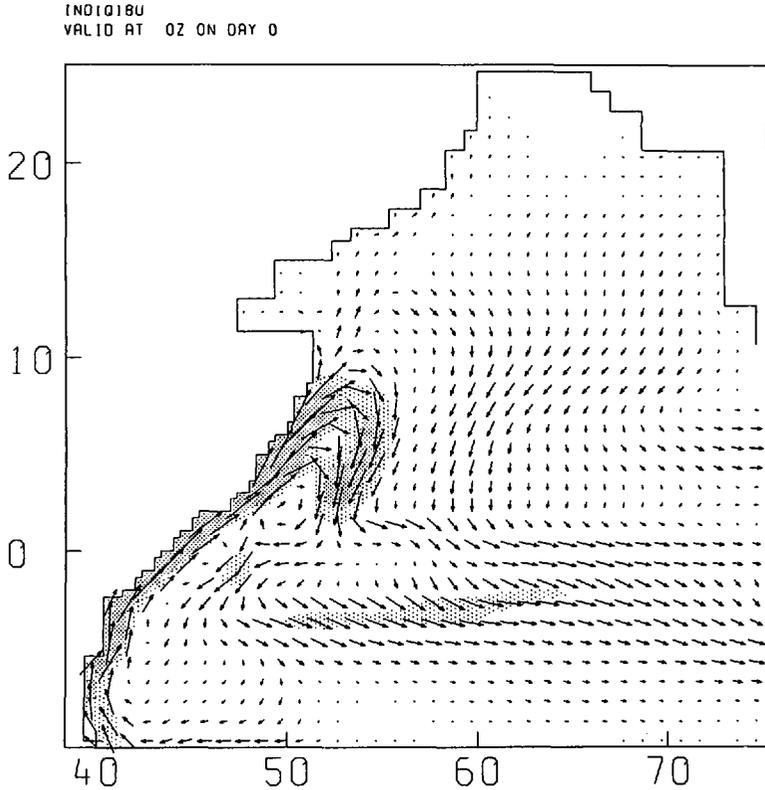


Figure 14. Currents for experiment IND1 for July at depths of (a) 35 m, (b) 48 m, and (c) 96 m, showing the cork screwing motion of the Somali gyre. Shading is as for Figure 5.

of a southern cold wedge partly because the flow does not separate completely from the coast. As the S-W monsoon weakens, the Great Whirl decays and moves northwards a little, but does not move rapidly northward as in Luther and O'Brien (1989). (Nor is it necessary to include the island of Socotra to keep the gyre from moving north during the S-W monsoon period as in Luther and O'Brien, but this does not argue that we should not include Socotra in subsequent integrations.)

The model used in the present study has a reasonable vertical resolution (8 levels in the top 165 m) and can resolve vertical structure which the layer models of MK and Luther and O'Brien cannot. In particular the importance of density changes within the flow round the gyres is illustrated. Flow at the surface along the boundary slides beneath the surface when the flow leaves the coast as illustrated by the cork-screw nature of the Great Whirl. This feature has not previously been noted and cannot be reproduced by the reduced gravity models nor the MK model. In no experiment did the model produce a northward movement of the low latitude separation. In reality, this is observed to happen late in the monsoon and Schott (1983) has argued that this is not connected to changes in the wind. The results of

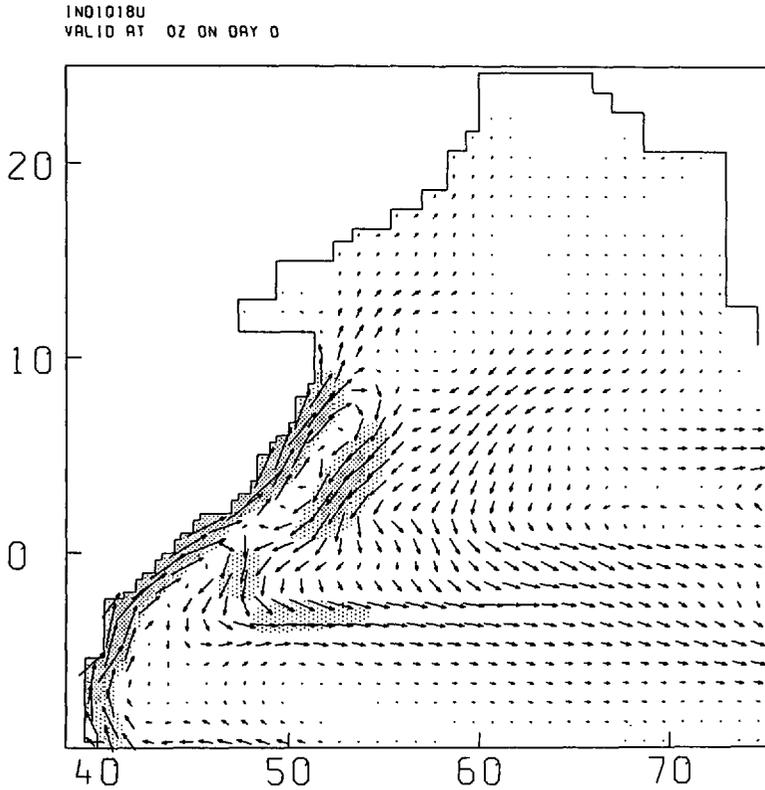


Figure 14. (Continued)

MK are consistent with that interpretation: the results of the GCM integration are not, but are consistent with those of Luther and O'Brien in this respect.

The cross-equatorial flow is shallow which seems to be consistent with the observations of Schott (1983). The separation of this flow from the coast and the attendant cold wedge seem to be quite sensitive to the stratification and are not very well reproduced in the seasonal-cycle integration. Either the sub-surface thermal structure is smoothed out over the 3 year period or the model upwelling does not reach deep enough.

Finally the nature of the secondary instabilities in the GCM seem to be different to those in, for example, the MK model. Whereas the MK model produces a coastal eddy to the north of the main gyre, the GCM response is to produce a series of jets to the east-north-east which can sometimes look a little like eddies. The reason for the different response between the GCM and layer model has not been resolved.

Acknowledgments. This work was supported under EC contract no EV4C 0042UK(H). Helpful comments were received from Julian McCreary and Mark Cane to whom the authors wish to express their appreciation.

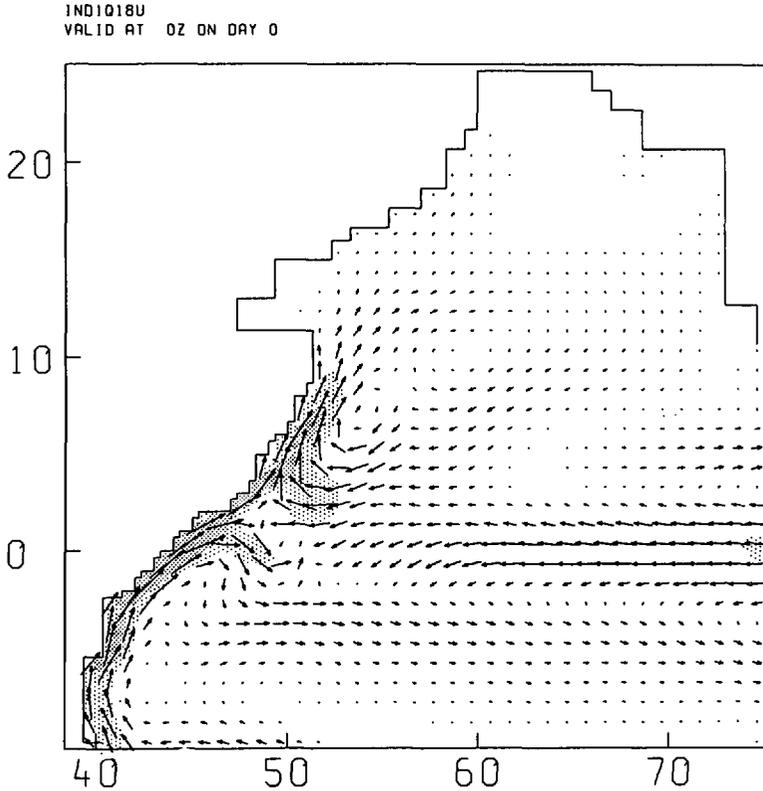


Figure 14. (Continued)

REFERENCES

- Anderson, D. L. T. and J. P. McCreary. 1985. Slowly propagating disturbances in a coupled ocean-atmosphere model. *J. Atmos. Sci.*, 42, 615-628.
- Anderson, D. L. T. and D. W. Moore. 1979. Cross equatorial inertial jets with special relevance to very remote forcing of the Somali Current. *Deep-Sea Res.*, 26, 1-22.
- Anderson, D. L. T. and P. Rowlands. 1976. The Somali Current response to the Southwest Monsoon: the relative importance of local and remote forcing. *J. Mar. Res.*, 34, 395-417.
- Brown, O., J. G. Bruce and R. H. Evans. 1980. Evolution of sea surface temperature in the Somali basin during the southwest Monsoon of 1979. *Science*, 209, 595-597.
- Bruce, J. G. 1981. Variations in the thermal structure and wind field occurring in the Western Indian Ocean during the monsoons. Naval Oceanographic Office Bay St. Louis, TR272.
- 1979. Eddies off the Somali coast during the Southwest Monsoons. *J. Geophys. Res.*, 84, 7742-7748.
- 1973. Large-scale variations of the Somali Current during the southeast Monsoon 1970. *Deep-Sea Res.*, 20, 837-846.
- Bruce, J. G. and G. Volkmann. 1969. Some measurements of current off the Somali coast during the northeast monsoon. *J. Geophys. Res.*, 74, 1958-1967.
- Bryan, K. 1969. A numerical method for the study of the circulation of the world ocean. *J. Comput. Phys.*, 4, 347-376.

- Cane, M. A. 1979. The response of an equatorial ocean to simple wind stress patterns II. Numerical results. *J. Mar. Res.*, *37*, 253–299.
- Carrington, D. J. 1990. An ocean general circulation model of the Indian Ocean for hindcasting studies. Climate Research Technical Note No 2. UK Met. Office, Bracknell.
- Cox, M. D. 1979. A numerical study of Somali Current eddies. *J. Phys. Oceanogr.*, *9*, 311–326.
- 1984. A primitive equation, 3-dimensional model of the ocean. GFDL Ocean Group Technical Report No. 1, GFDL/NOAA, Princeton, N.J.
- Düing, W., R. L. Molinari and J. C. Swallow. 1980. Somali Current: Evolution of surface flow. *Science*, *209*, 588–589.
- Esbensen, S. K. and Y. Kushnir. 1981. The heat budget of the global ocean: An atlas based on estimates from surface marine observations. Report No. 29, Climate Research Institute, Oregon State University, Corvallis.
- Findlater, J. 1971. Mean monthly airflow at low levels over the western Indian Ocean. *Geophysical Memoirs*, no. *115*, 53 pp.
- Findlay, A. G. 1866. A directory for the Navigation of the Indian Ocean. Richard Holmes Laurie, London, 1062 pp.
- Haney, R. L. 1971. Surface thermal boundary conditions for ocean models. *J. Phys. Oceanogr.*, *1*, 241–248.
- Hellerman, S. and M. Rosenstein. 1983. Normal monthly wind stress over the world ocean with error estimates. *J. Phys. Oceanogr.*, *13*, 1093–1104.
- Hurlburt, H. E. and J. D. Thomson. 1976. A numerical model of the Somali Current. *J. Phys. Oceanogr.*, *6*, 646–664.
- Jaeger, L. 1976. Monthly maps of precipitation for the whole world ocean. D. Wetterd., Ber. 18, Nr. 139, Offenbach.
- Kindle, John C. and J. Dana Thompson. 1989. The 26 and 50-day oscillations in the Western Indian Ocean Model results. *J. Geophys. Res.*, *94*, C4, 4721–4736.
- Knox, R. A. and D. L. T. Anderson. 1985. Recent advances in the study of the low-latitude ocean circulation. *Prog. Oceanogr.*, *14*, 259–317.
- Leetmaa, A., D. R. Quadfasel and D. Wilson. 1982. Development of the flow field during the onset of the Somali Current, 1979. *J. Phys. Oceanogr.*, *12*, 1325–1342.
- Levitus, S. 1982. Climatological atlas of the world ocean. NOAA Prof. Paper.
- Luther, M. E. 1987. Indian Ocean Modelling, *in* Further Progress in Equatorial Oceanography, E. J. Katz and J. M. Witte, eds., Nova Univ. Press.
- Luther, M. E. and J. J. O'Brien. 1985. A model of the seasonal circulation in the Arabian Sea forced by observed winds. *Prog. Oceanogr.*, *14*, 353–385.
- 1989. Modelling the variability in the Somali Current, *in* Mesoscale/Synoptic Coherent Structures in Geophysical Turbulence, J. Nihoul and B. Jamart, eds., Elsevier.
- Luther, M. E., J. J. O'Brien and A. H. Meng. 1985. Morphology of Somali Current system during the southwest monsoon. Coupled Ocean-Atmosphere Models J. C. J. Nihoul, ed., Elsevier Oceanography series. 405–436.
- McCreary, J. P. and P. K. Kundu. 1988. A numerical investigation of the Somali Current during the Southwest Monsoon. *J. Mar. Res.*, *46*, 25–58.
- Pacanowski, R. C. and S. G. H. Philander. 1981. Parameterization of vertical mixing in numerical models of tropical oceans. *J. Phys. Oceanogr.*, *11*, 1443–1451.
- Paulson, C. A. and J. J. Simpson. 1977. Irradiance measurements in the upper ocean. *J. Phys. Oceanogr.*, *7*, 952–956.
- Philander, S. G. H. and P. Delecluse. 1983. Coastal currents in low latitudes. *Deep-Sea Res.*, *30*, 887–902.

- Schott, F. 1983. Monsoon response of the Somali Current and associated upwelling. *Prog. Oceanogr.*, *12*, 357–381.
- Schott, Fredrich, Michele Fieux, John Kindle, John Swallow and Rainer Zantopp. 1988. The Boundary Currents east and north of Madagasiar 2. Direct Measurements. *J. Geophys. Res.*, *93*, C5, 4963–4974.
- Swallow, J. C. and J. G. Bruce. 1966. Current measurements off the Somali coast during the southwest monsoon of 1964. *Deep-Sea Res.*, *13*, 861–888.
- Swallow, J. C. and M. Fieux. 1982. Historical evidence for two gyres in the Somali Current. *J. Mar. Res.*, *40* (Suppl.), 747–755.
- Swallow, J. C., Robert L. Molinari, John G. Bruce, Otis B. Brown and Robert Evans. 1983. Development of near-surface flow pattern and water mass distribution in the Somali Basin in response to the Southwest Monsoon of 1979. *J. Phys. Oceanogr.*, *13*, 1398–1415.
- Woodberry, Karen E., Mark Luther and James J. O'Brien. 1989. The wind-driven seasonal circulation in the Southern tropical Indian Ocean. *J. Geophys. Res.*, *94*, C12, 17985–18002.
- Wyrtki, K. 1973. An equatorial jet in the Indian Ocean. *Science*, *181*, 262–264.